pipette. After 32 h, the cells were fixed with 3.7% formaldehyde in PBS for 20 min, and pictures of the wound were taken at the different field.

Soft Agar Colonogenic Assay. Soft agar assay was performed by seeding the cells at a density of 1×10^4 in a 60-mm diameter tissue culture dish containing 0.33% top low-melt agarose-0.6% bottom low-melt agarose. Cells were fed every 3 days. Colonies were counted and measured after 2 weeks.

Gene Reporter Assays. A total of 2×10^5 cells was seeded in each well of a 6-well dish and transfected with desired plasmids using Lipofectamine 2000 reagent (Invitrogen). The assays were performed with the dual luciferase reporter assay system from Promega. The internal controls used were pRL-TK and pRL-CMV to track transfection efficiency. The cells were harvested after 48 h. Each data point obtained is the mean of three independent experiments.

Xenograft Studies. EJ-HB-EGF and EJ-CAT cells were cultured in media with and without tet for 24 h. Cells were washed twice with DMEM without antibiotics and serum and finally resuspended at a density of 2×10^6 cells in 0.25 ml. The cell suspension was injected s.c. (bilaterally, 0.25 ml/site) into 6-week-old nude athymic mice [Taconic; Cr:(NCr)-nu f BR]. HB-EGF expression was suppressed by feeding mice with water containing 500 μg of doxycycline (dox)/ml in 1% sucrose. Mice were killed after 3 weeks. Tumors were excised and weighed, fixed for 1 h in 10% formalin, washing with PBS, followed by embedding in ornithine carbamyl transferase, and frozen in liquid nitrogen. Six mice were used for each sample.

Computer-Assisted Morphometric Analysis of Intratumoral Vasculature. Representative tumor sections were stained with anti-CD31 mouse monoclonal antibodies to visualize the blood vessels. Six tumors were evaluated/each sample, and five areas were evaluated at ×6 magnification. Images were captured with a Spot digital camera (Diagnostic Instruments, Sterling Heights, MI), and blood vessels were quantified using IPLab software (Scanalytics, Billerica, MA). The two-sided unpaired *t* test was used to analyze differences in microvessel density and vascular size and area.

RESULTS

Effects of HB-EGF on the Transformed Phenotype. To elucidate the role of HB-EGF overexpression in the process of tumorigenesis in human cancer cells, a tet-regulated HB-EGF-inducible system was generated in EJ cells that contain a low basal level of HB-EGF. Three different forms (wt-, s-, and pro-HB-EGF) of HB-EGF expression induced by the removal of tet resulted in an increase of each form of HB-EGF (Fig. 1*A*). Using this system, we first examined the role of HB-EGF in cell proliferation. The growth rate of EJ-HB-EGF cells was measured in the presence or absence of tet at 1×10^4 cells in 6-well plates for up to 8 days. Induction of wt- or s-HB-EGF by removal of tet resulted in a substantial growth rate increase, as seen by the 75–100% increase, when compared with HB-EGF-repressed cells (tet+; Fig. 1*B*). However, pro-HB-EGF induction in EJ cells resulted in a slight increase of growth rate by ~25%. To examine the effect of HB-EGF on cell colony formation ability, EJ-HB-EGF cells expressing three different types of HB-EGF were seeded at 200 cells/100-mm diameter dish. Cells expressing s- or wt-HB-EGF produced approximately two to three times more colonies than that of pro-HB-EGF-induced cells (Fig. 1*C*). We next evaluated the effect of each HB-EGF on colony formation in soft agarose as an additional measure of tumorigenicity *in vitro* using tet-regulated EJ-HB-EGF cells. The results of agar colony tests are shown in Fig. 1*D*. Soluble- or wt-HB-EGF (tet-)-inducing cells significantly stimulated anchorage-independent growth, but anchorage-independent growth was not seen in pro-HB-EGF-induced cells. A colony formation assay in soft agarose was also used to examine whether HB-EGF could promote a transformed phenotype in a different cell line using HeLa cells. Transfection of HeLa cells with wt- or s-HB-EGF following a selection under G418 significantly increased sizes of colonies in soft agarose as compared with those in cells transfected with vector alone or a plasmid expressing pro-HB-EGF (Fig. 1*E*). Taken together, these results suggest that s-HB-EGF expression causes an enhanced transformed phenotype *in vitro* but pro-HB-EGF overexpression does not.

s-HB-EGF Elevates Cyclin D Expression via Cyclin D Promoter. It is well known that the signaling pathways of oncogenes, including ErbB2 and Ras, can up-regulate cyclin D expression. Recent

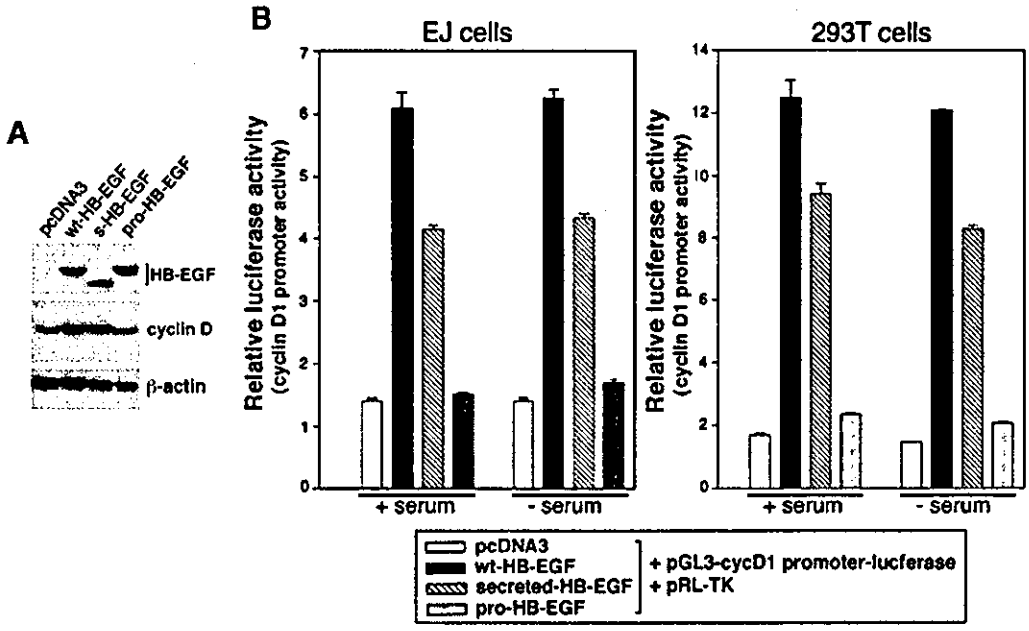

Fig. 2. Soluble heparin-binding epidermal growth factor-like growth factor (s-HB-EGF) elevates the cyclin D1 protein level and activates the cyclin D1 promoter. *A*, increase in cellular cyclin D1 protein by s- or wild-type (wt)-HB-EGF. Tetracycline (tet)-regulated EJ-HB-EGF cells were cultured in the absence or presence of tet followed by an immunoblot analysis of the cell lysates with antibodies against HB-EGF, cyclin D1, and β-actin (loading control). *B*, activation of cyclin D1 promoter by HB-EGF. EJ cells were transiently cotransfected with the cyclin D1 promoter reporter construct (−1745CD1) and three different forms of HB-EGF [wt-HB-EGF, s-HB-EGF, and membrane-anchored form (pro)-HB-EGF] in expression vector, respectively, or the empty vector then assayed for luciferase activity. pRL-TK Renilla luciferase reporter construct was cotransfected with each sample to normalize transfection efficiency. All results are expressed as x ± SD of three independent experiments with duplicates.

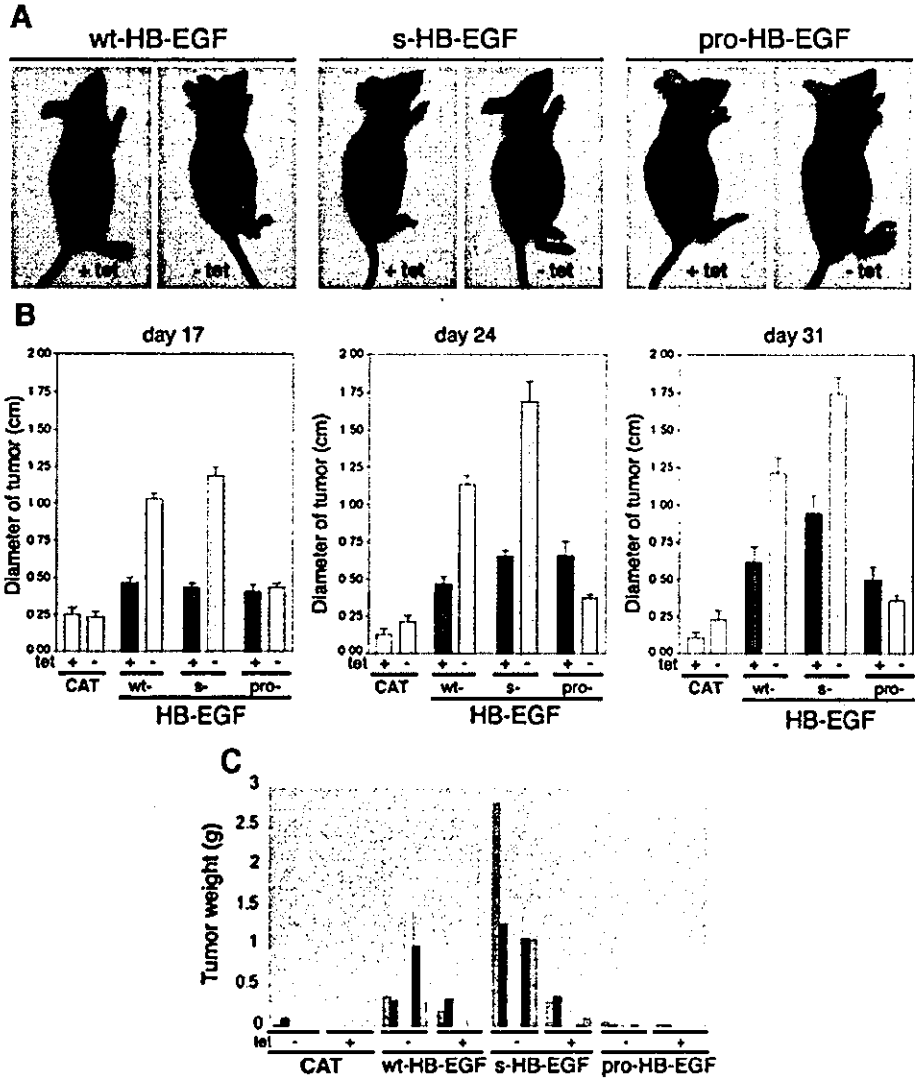

Fig. 3. Soluble heparin-binding epidermal growth factor-like growth factor (s-HB-EGF) overexpression increases tumorigenicity in nude mice. *A*, athymic nude mice received injections of 2×10^6 EJ-s-HB-EGF cells, EJ-wt-HB-EGF, EJ-pro-HB-EGF, or EJ-CAT cells mixed with an equal volume of Matrigel. The cell suspension was injected s.c. (bilaterally; 0.5 ml/site) into nude mice. Results are average tumor sizes for six animals into a site/experimental condition 3 weeks after injection. *B*, the mean tumor size of s- or wild-type (wt)-HB-EGF expressing EJ cells (−tet EJ-s-HB-EGF) was significantly larger than that of the EJ-CAT tumor (−tet EJ-CAT), EJ-pro-HB-EGF tumor (−tet EJ-pro-HB-EGF), or that of EJ-s-HB-EGF or EJ-wt-HB-EGF tumor from mice fed with doxycycline (500 μg/ml in water) to repress all forms of HB-EGF expression. *C*, representation of the mean tumor weight.

studies demonstrate that HB-EGF activates MAPK cascade through the activation of the Ras/Raf pathway (34). Therefore, we tested whether HB-EGF had any effect on cyclin D expression. To examine this possibility, we transiently transfected three different HB-EGF expression constructs, respectively, into EJ cells and then examined the effects on endogenous cyclin D1 levels. Forced expression of s- or wt-HB-EGF led to ~3-fold increase in cyclin D1 protein levels, whereas pro-HB-EGF did not result in an increase in cyclin D expression. (Fig. 2*A*). To determine whether HB-EGF regulates the transcription of cyclin D1, we also measured the effects of HB-EGFs on the cyclin D1 promoter using a cyclin D1-luciferase reporter construct (−1745CD1; Ref. 35). The reporter containing the cyclin D promoter was strongly activated in response to the expression of s- or wt-HB-EGF in EJ cells and 293T cells (Fig. 2*B*), whereas pro-HB-EGF did not show any significant effect on cyclin D promoter activity, regardless of serum presence. These results indicate that the activation of the cyclin D promoter and the −1745CD1 promoter fragment retains complete responsiveness to s-HB-EGF.

HB-EGF Overexpression Promotes Cancer Cell Growth *in Vivo*. To determine whether HB-EGF increases tumorigenicity *in vivo*, xenograft studies were conducted using EJ cells expressing s-HB-EGF, wt-HB-EGF, and pro-HB-EGF, respectively, and control cells expressing CAT (EJ-CAT) in the absence or presence of dox. Six mice per each HB-EGF form were injected with cells (2×10^6 cells mixed with Matrigel). As shown in Fig. 3, *A* and *B*, EJ cells expressing s- or wt-HB-EGF showed an increased overall tumor size when injected into nude athymic mice (EJ-HB-EGF tumors in −tet condition), compared with EJ cells expressing a control CAT protein (EJ-CAT tumors in −tet and +tet) and EJ-HB-EGF cells in tet+ conditions. The mean size of EJ-HB-EGF tumors maintained in the absence of dox was 1.5 g, significantly larger than tumors from control mice, ~0.1 g (Fig. 3*C*). However, tumors expressing pro-HB-EGF were similar to those of control mice. Data from the *in vitro* tumorigenicity assays and the xenograft assays support the conclusion that s-HB-EGF exerts a potent oncogenic potential but pro-HB-EGF does not.

HB-EGF Overexpression in Bladder Carcinomas Up-Regulates VEGF and Enhances Tumor Angiogenesis in Mice. The growth of tumors beyond a minimal size has been hypothesized to be dependent upon the induction of new blood vessel growth or angiogenesis, which in turn supplies needed nutrients to rapidly dividing tumor cells (36). Several studies indicated that HB-EGF can be up-regulated in some pathological states that may involve angiogenesis (37, 38). Some studies showed that VEGF, a critical factor in the development of new blood vessels, could induce HB-EGF in vascular endothelial cells and speculated that HB-EGF induction by VEGF may act in a paracrine fashion to promote angiogenesis (39). This prompted us to evaluate

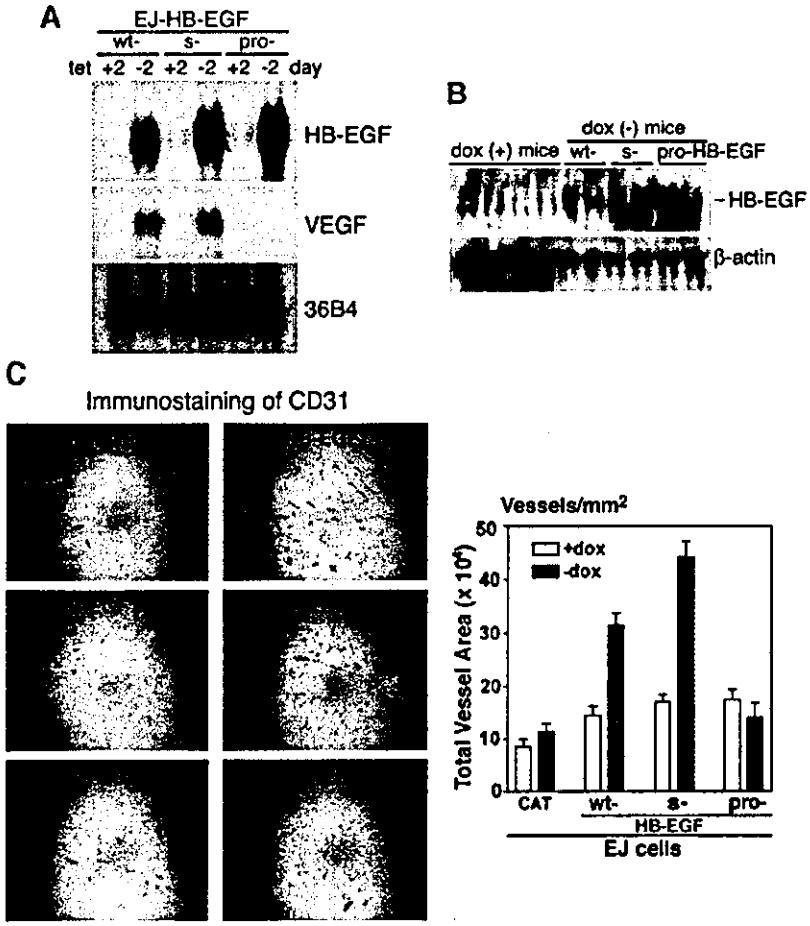

Fig. 4. Heparin-binding epidermal growth factor-like growth factor (HB-EGF) increases tumor angiogenesis in nude mice. *A*, up-regulation of vascular endothelial growth factor (VEGF) by HB-EGF induction in EJ cells. Induction of VEGF mRNA after tetracycline removal in EJ-s- or wt-HB-EGF cells. Total RNA was prepared from EJ-HB-EGF cells grown in the presence or absence of tet for 2 days. Northern blot analyses were performed sequentially using a ^{32}P-labeled probe against HB-EGF, VEGF, and 36B4 (loading control). *B*, Western blot analysis of HB-EGF expressing tumors (−dox mice) or control tumors (+dox mice). Three weeks after injection, tumors were harvested, homogenized and examined for HB-EGF expression by Western blotting. *C*, immunostaining of CD31. Immunostaining of anti-CD31 (PECAM-1) monoclonal antibody demonstrated rarefication of tumor blood vessels in HB-EGF-overexpressing tumors as compared with control tumors (+/−CAT and +dox). *Bar* = 100 μm. CD31-stained blood vessels were evaluated in three different ×10 fields obtained from five different tumors for each condition. *Right panel* represents quantitative computer-assisted image analysis that revealed a significant increase of angiogenesis in soluble (s)- or wild-type (wt)-HB-EGF-overexpressing EJ tumors but not in membrane-anchored form (pro)-HB-EGF tumors, as measured by the number of blood vessels/mm^2 tumor area.

the effect of HB-EGF on the existence of a growth factor-mediated autocrine response, possibly involving VEGF up-regulation. Northern blot analysis was performed with total RNA from EJ cells with a tet-regulated HB-EGF-inducible system. Soluble-HB-EGF or wt-HB-EGF expression by removal of tet resulted in an increase of VEGF mRNA (Fig. 4*A*), but no increase of VEGF mRNA by pro-HB-EGF induction in EJ-pro-HB-EGF cells was seen. These results implicate the up-regulation of HB-EGF as an angiogenesis-related change, occurring through an autocrine response, which is closely associated with tumorigenesis of epithelial cells.

Next, we examined the effect of HB-EGFs on blood vessel growth/angiogenesis in mice. Three weeks after injection, tumors harvested from control and three forms of HB-EGF-expressing mice in the xenograft studies (Fig. 3) were first homogenized and examined for HB-EGF expression levels by Western blotting. Fig. 4*B* shows that mice maintained in the absence of dox-expressed HB-EGF at a higher level as compared with dox-fed mice. Cryostat sections of five different tumors expressing HB-EGF for each experimental condition include the following: +dox of EJ-HBEGF (no HB-EGF expression); −dox of EJ-HBEGF (HB-EGF expressed); +dox and −dox of EJ-CAT cells were processed and stained for CD31 (PECAM-1), an endothelial junction molecule (40). As shown in Fig. 4*C*, these sections demonstrated a dramatic increase of microvessels in s- or wt-HB-EGF expressing tumors (+wt-HB-EGF and +s-HB-EGF, -dox) when compared with the different control tumors (+dox, +CAT and −CAT, and +pro-HB-EGF). To achieve a more detailed quantification of the effects of HB-EGF on tumor angiogenesis, average vessel density, vessel size, and percentage of tissue area covered by vessels were determined by computer-assisted image analysis of representative digital images. The relative tumor area occupied by vessels increased ~2–3-folds in s- or wt-HB-EGF-expressing tumors (Fig. 4*C*, *right panel*).

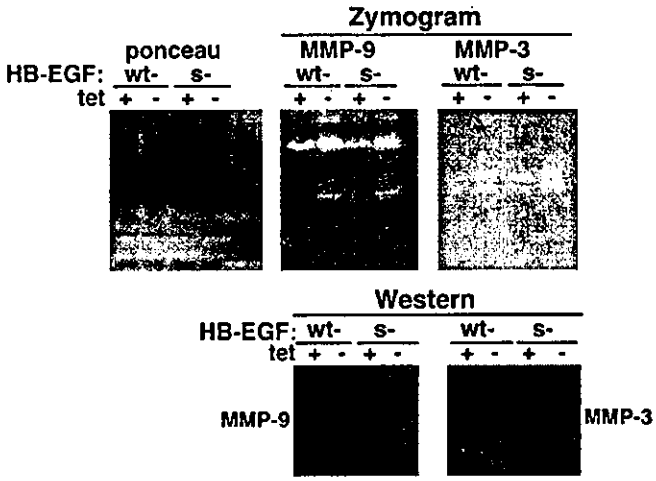

Fig. 5. Up-regulation of metalloprotease (MMP)-9 and MMP-3 in response to heparin-binding epidermal growth factor-like growth factor (HB-EGF) induction. EJ-HB-EGF cells expressing soluble (s)-, wild-type (wt)-, and membrane-anchored form (pro)-HB-EGF were grown in the absence or presence of tetracycline (tet) for 48 h, respectively, then analyzed by zymography for MMP-9 and MMP-3 activities. Expression levels of MMP-9 and MMP-3 were also determined by Western blotting. Ponceau staining shows the loading levels of total proteins.

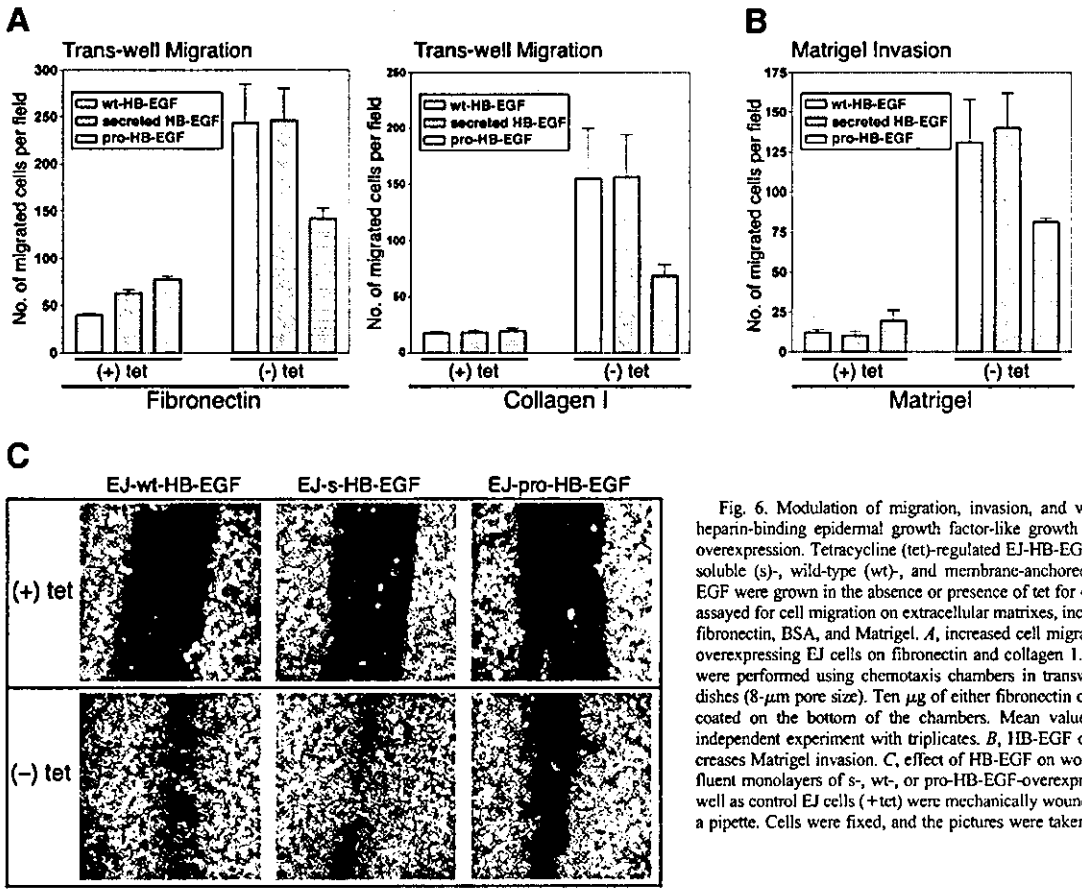

Fig. 6. Modulation of migration, invasion, and wound healing by heparin-binding epidermal growth factor-like growth factor (HB-EGF) overexpression. Tetracycline (tet)-regulated EJ-HB-EGF cells expressing soluble (s)-, wild-type (wt)-, and membrane-anchored form (pro)-HB-EGF were grown in the absence or presence of tet for 48 h, respectively, assayed for cell migration on extracellular matrixes, including collagen 1, fibronectin, BSA, and Matrigel. *A*, increased cell migration of HB-EGF-overexpressing EJ cells on fibronectin and collagen 1. Migration assays were performed using chemotaxis chambers in transwell tissue culture dishes (8-μm pore size). Ten μg of either fibronectin or collagen 1 were coated on the bottom of the chambers. Mean values ± SD of two independent experiment with triplicates. *B*, HB-EGF overexpression increases Matrigel invasion. *C*, effect of HB-EGF on wound healing. Confluent monolayers of s-, wt-, or pro-HB-EGF-overexpressing EJ cells as well as control EJ cells (+tet) were mechanically wounded with the tip of a pipette. Cells were fixed, and the pictures were taken after 32 h.

Up-Regulation of the MMP by HB-EGF. It is well documented that the up-regulation of MMP activities results in the proteolytic degradation of the extracellular matrix and the basement membrane, which promotes tumor growth and metastasis (41). To better evaluate the participation of HB-EGF in tumor migration and progression, we tested the effects of HB-EGF on MMP-9 activation. As shown in Fig. 5, HB-EGF induction after tet removal activated the 92-kDa pro-MMP-9 zymogen to the 67-kDa active form. The processing/activation was analyzed by zymography analysis. MMP-9 expression level was also determined by Northern and Western blotting, which showed that MMP-9 levels correlated with an increase of HB-EGF levels (Fig. 5). MMP-3, also known as a stromelysin-1, is the most efficient activator of MMP-9 *in vitro* and *in vivo*. Therefore, we evaluated the effect of HB-EGF on MMP-3 activity. Fig. 5 also shows the slightly increased activation and expression of MMP-3 in response to HB-EGF induction. However, HB-EGF-mediated activation of MMP-9 was not observed in response to pro-HB-EGF overexpression (data not shown). These results demonstrate that the expression level and activity of MMP-9 and MMP-3 can be enhanced in response to s-HB-EGF in EJ cells.

HB-EGF Effect on Migration and Wound Healing. We next investigated whether HB-EGF might be involved in extracellular matrix interactions in EJ cells and cause an increase in the migration of cells expressing HB-EGF because HB-EGF has been shown to be chemotactic (1, 12, 42) and to mediate migration in some cell types (12). Tet-regulated EJ-HB-EGF cells were used for migration assays in a transwell migration assay (haptotaxis). We tested for their ability to migrate through extracellular matrixes, including fibronectin, collagen 1, and Matrigel. As shown in Fig. 6*A*, HB-EGF expression in EJ cells after the removal of tet showed a strong increase in migration on all three substrates but not in cells grown in the presence of tet. Although s-HB-EGF and wt-HB-EGF were more effective, pro-HB-EGF expression also increased cell migration on all three matrixes.

It is well established that successful wound healing involves a number of processes, including cell proliferation, cell migration, vascular permeability, and angiogenesis (43). HB-EGF is known to be up-regulated in the wound-healing process of certain cell types, including keratinocytes (44, 45). Because HB-EGF expression triggers tumor angiogenesis and cell migration in EJ cells, we studied its effect on wound healing using the same cell system. One $\times 10^6$ EJ-HB-EGF cells of each form (EJ-wt-HB-EGF, EJ-s-HB-EGF, and pro-HB-EGF) were seeded in a 6-well plate. Then, the cells were grown with or without tet for 24 h. A wound was introduced by the use of a pipette tip. After 32 h, the cells were fixed, and pictures were taken at different regions of the wound (Fig. 6*C*). Soluble- or wt-HB-EGF expression (−tet condition) increased the effectiveness of wound healing, but no significant effect was seen in pro-HB-EGF-expressing cells.

DISCUSSION

In this article, we provide evidence that HB-EGF exerts oncogenic potentials *in vitro* and *in vivo*. We found that overexpression of HB-EGF enhanced the transformed phenotype *in vitro* as determined by cell proliferation, anchorage-independent growth, and foci formation assays. We also showed that HB-EGF can activate the cyclin D promoter. We established a tet-regulated HB-EGF expression system using three different forms of HB-EGF in EJ human bladder cancer cells to test the tumorigenicity *in vitro* and *in vivo* using a xenograft assay. Inducible overexpression of s- or wt-HB-EGF caused increased

tumor formation in mice, supporting the conclusion that s-HB-EGF but not the membrane-bound form of HB-EGF exerts a potent oncogenic ability. Our finding that the membrane-bound form of HB-EGF does not exert oncogenic potential may support previous speculation that pro-HB-EGF may act as a negative regulator of cell proliferation (46).

HB-EGF is known as a potent mitogen for keratinocytes, hepatocytes, smooth muscle cells, and fibroblasts (2, 29, 44). HB-EGF expression is elevated in human cancers, including hepatocellular and gastric carcinoma, breast carcinoma, melanoma, colon cancer, pancreatic cancer, glioma and glioblastoma (23, 24). Furthermore, HB-EGF is induced in NIH3T3 cells transformed by v-Ras or v-Raf (34). HB-EGF was identified as a target of v-Jun, a potent oncogene, and HB-EGF plays a role in v-Jun-mediated oncogenic transformation (15). The significance of HB-EGF overexpression in tumorigenesis is also supported by our findings that HB-EGF activates the cyclin D promoter, implying that v-Jun could stimulate cyclin D transcription through HB-EGF induction. We have previously reported the identification of *HB-EGF* as a p53 downstream target gene, and p53 induction of HB-EGF could activate cell survival signaling, including AKT and MAPK cascades (19). A recent article has demonstrated that inducible expression of oncogenic Raf in normal epithelial cells strongly induced autocrine expression of HB-EGF, transforming growth factor α, and amphiregulin, which were directly implicated in the ability of sustained Raf/MAPK pathway stimulation to protect cells from apoptosis (47).

It is now well established that VEGF is an endothelial cell-specific, multifunctional growth factor that plays a major role in the initiation of angiogenesis by acting directly as a mitogenic and chemotactic factor (48). Although HB-EGF is known to have no effect on the proliferation of endothelial cells, some studies demonstrated that VEGF induces expression of angiogenic growth factors, including HB-EGF, in vascular endothelial cells and suggested that HB-EGF induction in response to VEGF provides a critical endothelial cell-derived signal, perhaps the activation of the MAPK and AKT cascade, for the process of new blood vessel formation and maturation (39). In addition, the reviews have proposed that HB-EGF acts as one of the recruiting signals for mesenchymal cells during the late phase of angiogenesis (49), implying that HB-EGF plays a critical role in angiogenesis as well as tumor development. In this study, we also demonstrate that s- or wt-HB-EGF induces VEGF expression, whereas it inhibits thrombospondin-1 expression (data not shown), implying the presence of an autocrine growth factor stimulation. Moreover, HB-EGF promotes tumor angiogenesis *in vivo* and exerts the migration-stimulating and wound-healing potential for cancer cells.

It is now clear that the up-regulation of MMP activities results in the proteolytic degradation of the extracellular matrix and the basement membrane, which promotes tumor growth, angiogenesis, and metastasis (41). It is possible that the effect of HB-EGF on the functional interaction between VEGF and MMP-9 is a key mechanism for initiation and maintenance of angiogenesis. In our cell system, we found a significant difference in the levels of active MMP-9 and MMP-3 in s-HB-EGF-induced cells. Moreover, recent studies clearly demonstrated that MMP-9 mediates the release and accumulation of VEGF from the cell matrix and that MMP-9 triggers the angiogenic switch (50). The generation of HB-EGF overexpressing mice or a targeted deletion of HB-EGF should provide additional understanding of mechanisms underlying HB-EGF-associated functions in angiogenesis.

In summary, our findings provide evidence that HB-EGF enhances transformed phenotypes and is associated with the stimulation of MMP-9, MMP-3, and cyclin D activation, which promotes tumorigenesis and angiogenesis. Given its elevated expression in human cancers along with our findings of HB-EGF contribution to enhanced transformed phenotypes, we hypothesize that HB-EGF may behave as an oncogene and, as such, could have importance as a therapeutic target.

ACKNOWLEDGMENTS

We thank Michael Klasbrun for providing wt-HB-EGF cDNA, Rachel Hazan, Don Senger, Jeremy Brown, and Shanthy Nuti for helpful discussion, and Paula Velasco for technical help. We also thank Wendy Wong for technical help.

REFERENCES

1. Raab G, Klagsbrun M. Heparin-binding EGF-like growth factor. Biochim Biophys Acta 1997;1333:F179–99.
2. Higashiyama S, Abraham JA, Miller J, Fiddes JC, Klagsbrun MA. Heparin-binding growth factor secreted by macrophage-like cells that is related to EGF. Science (Wash. DC) 1991;251:936–9.
3. Blotnick S, Peoples GE, Freeman MR, Eberlein TJ, Klagsbrun MT. Lymphocytes synthesize and export heparin-binding epidermal growth factor-like growth factor and basic fibroblast growth factor, mitogens for vascular cells and fibroblasts: differential production and release by CD4+ and CD8+ T cells. Proc Natl Acad Sci USA 1994;91:2890–4.
4. Fukuda K, Inui Y, Kawata S, et al. Increased mitogenic response to heparin-binding epidermal growth factor-like growth factor in vascular smooth muscle cells of diabetic rats. Arterioscler Thromb Vasc Biol 1995;15:1680–7.
5. Dluz SM, Higashiyama S, Damm D, Abraham JA, Klagsbrun M. Heparin-binding epidermal growth factor-like growth factor expression in cultured fetal human vascular smooth muscle cells. Induction of mRNA levels and secretion of active mitogen. J Biol Chem 1993;268:18330–4.
6. Graus-Porta D, Beerli RR, Daly JM, Hynes NE. ErbB-2, the preferred heterodimerization partner of all ErbB receptors, is a mediator of lateral signaling. EMBO J 1997;16:1647–55.
7. Iwamoto R, Mekada E. Heparin-binding EGF-like growth factor: a juxtacrine growth factor. Cytokine Growth Factor Rev 2000;11:335–44.
8. Hisaka T, Yano H, Haramaki M, Utsunomiya I, Kojiro M. Expressions of epidermal growth factor family and its receptor in hepatocellular carcinoma cell lines: relationship to cell proliferation. Int J Oncol 1999;14:453–60.
9. Murayama Y, Miyagawa J, Shinomura Y, et al. Significance of the association between heparin-binding epidermal growth factor-like growth factor and CD9 in human gastric cancer. Int J Cancer 2002;98:505–13.
10. Nakamura Y, Handa K, Iwamoto R, Tsukamoto T, Takahasi M, Mekada E. Immunohistochemical distribution of CD9, heparin binding epidermal growth factor-like growth factor, and integrin alpha$_3$beta$_1$ in normal human tissues. J Histochem Cytochem 2001;49:439–44.
11. Hashimoto K, Higashiyama S, Asada H, et al. Heparin-binding epidermal growth factor-like growth factor is an autocrine growth factor for human keratinocytes. J Biol Chem 1994;269:20060–6.
12. Nishi E, Prat A, Hospital V, Elenius K, Klagsbrun M. *N*-Arginine dibasic convertase is a specific receptor for heparin-binding EGF-like growth factor that mediates cell migration. EMBO J 2001;20:3342–50.
13. Suo Z, Risberg B, Karlsson MG, Villman K, Skovlund E, Nesland JM. The expression of EGFR family ligands in breast carcinomas. Int J Surg Pathol 2002;10:91–9.
14. Tarbe N, Losch S, Burtscher H, Jarsch M, Weidle UH. Identification of rat pancreatic carcinoma genes associated with lymphogenous metastasis. Anticancer Res 2002;22:2015–27.
15. Fu S, Bottoli I, Goller M, Vogt PK. Heparin-binding epidermal growth factor-like growth factor, a v-Jun target gene, induces oncogenic transformation. Proc Natl Acad Sci USA 1999;96:5716–21.
16. McCarthy SA, Chen D, Yang BS, et al. Rapid phosphorylation of Ets-2 accompanies mitogen-activated protein kinase activation and the induction of heparin-binding epidermal growth factor gene expression by oncogenic Raf-1. Mol Cell Biol 1997;17:2401–12.
17. Martinez-Lacaci I, De Santis M, Kannan S, et al. Regulation of heparin-binding EGF-like growth factor expression in Ha-ras transformed human mammary epithelial cells. J Cell Physiol 2001;186:233–42.
18. Fang L, Li G, Liu G, Lee SW, Aaronson SA. p53 induction of heparin-binding EGF-like growth factor counteracts p53 growth suppression through activation of MAPK and PI3K/Akt signaling cascades. EMBO J 2001;20:1931–9.
19. Miyoshi E, Higashiyama S, Nakagawa T, Hayashi N, Taniguchi N. Membrane-anchored heparin-binding epidermal growth factor-like growth factor acts as a tumor survival factor in a hepatoma cell line. J Biol Chem 1997;272:14349–55.
20. Downing MT, Brigstock DR, Luquette MH, Crissman-Combs M, Besner GE. Immunohistochemical localization of heparin-binding epidermal growth factor-like growth factor in normal skin and skin cancers. Histochem J 1997;29:735–44.
21. Fishman S, Brill S, Papa M, Halpern Z, Zvibel I. Heparin-derived disaccharides modulate proliferation and Erb-B2-mediated signal transduction in colon cancer cell lines. Int J Cancer 2002;99:179–84.

22. Ito Y, Takeda T, Higashiyama S, Noguchi S, Matsuura N. Expression of heparin-binding epidermal growth factor-like growth factor in breast carcinoma. Breast Cancer Res Treat 2001;67:81–5.
23. Ito Y, Takeda T, Higashiyama S, et al. Expression of heparin binding epidermal growth factor-like growth factor in hepatocellular carcinoma: an immunohistochemical study. Oncol Rep 2001;8:903–7.
24. Jayne DG, Perry SL, Morrison E, Farmery SM, Guillou PJ. Activated mesothelial cells produce heparin-binding growth factors: implications for tumour metastases. Br J Cancer 2000;82:1233–8.
25. Kim J, Adam RM, Freeman MR. Activation of the Erk mitogen-activated protein kinase pathway stimulates neuroendocrine differentiation in LNCaP cells independently of cell cycle withdrawal and STAT3 phosphorylation. Cancer Res 2002;62: 1549–54.
26. Thogersen VB, Sorensen BS, Poulsen SS, Orntoft TF, Wolf H, Nexo E. A subclass of HER1 ligands are prognostic markers for survival in bladder cancer patients. Cancer Res 2001;61:6227–33.
27. Wang YD, De Vos J, Jourdan M, et al. Cooperation between heparin-binding EGF-like growth factor and interleukin-6 in promoting the growth of human myeloma cells. Oncogene 2002;21:2584–92.
28. Kobrin MS, Funatomi H, Friess H, Buchler MW, Stathis P, Korc M. Induction and expression of heparin-binding EGF-like growth factor in human pancreatic cancer. Biochem Biophys Res Commun 1994;202:1705–9.
29. Ito N, Kawata S, Tamura S, et al. Heparin-binding EGF-like growth factor is a potent mitogen for rat hepatocytes. Biochem Biophys Res Commun 1994;198:25–31.
30. Sato M, Narita T, Kawakami-Kimura N, et al. Increased expression of integrins by heparin-binding EGF like growth factor in human esophageal cancer cells. Cancer Lett 1996;102:183–91.
31. Ruck A, Paulie S. EGF, TGF alpha, AR and HB-EGF are autocrine growth factors for human bladder carcinoma cell lines. Anticancer Res 1998;18:1447–52.
32. Murayama Y, Miyagawa J, Higashiyama S, et al. Localization of heparin-binding epidermal growth factor-like growth factor in human gastric mucosa. Gastroenterology 1995;109:1051–9.
33. Higashiyama S, Lau K, Besner GE, Abraham JA, Klagsbrun M. Structure of heparin-binding EGF-like growth factor. Multiple forms, primary structure, and glycosylation of the mature protein. J Biol Chem 1992;267:6205–12.
34. McCarthy SA, Samuels ML, Pritchard CA, Abraham JA, McMahon M. Rapid induction of heparin-binding epidermal growth factor/diphtheria toxin receptor expression by Raf and Ras oncogenes. Genes Dev 1995;9:1953–64.
35. Wulf GM, Ryo A, Wulf GG, et al. Pin1 is overexpressed in breast cancer and cooperates with Ras signaling in increasing the transcriptional activity of c-Jun towards cyclin D1. EMBO J 2001;20:3459–72.
36. Folkman J. Tumor angiogenesis: therapeutic implications. N Engl J Med 1971;285: 1182–6.
37. Abramovitch R, Neeman M, Reich R, et al. Intercellular communication between vascular smooth muscle and endothelial cells mediated by heparin-binding epidermal growth factor-like growth factor and vascular endothelial growth factor. FEBS Lett 1998;425:441–7.
38. Abramovitch R, Marikovsky M, Meir G, Neeman M. Stimulation of tumour growth by wound-derived growth factors. Br J Cancer 1999;79:1392–8.
39. Arkonac BM, Foster LC, Sibinga NE, et al. Vascular endothelial growth factor induces heparin-binding epidermal growth factor-like growth factor in vascular endothelial cells. J Biol Chem 1998;273:4400–5.
40. Skobe M, Hawighorst T, Jackso DG, et al. Induction of tumor lymphangiogenesis by VEGF-C promotes breast cancer metastasis. Nat Med 2001;7:192–8.
41. Egeblad M, Werb Z. New functions for the matrix metalloproteinases in cancer progression. Nat Rev Cancer 2002;2:161–74.
42. Elenius K, Paul S, Allison G, Sun J, Klagsbrun M. Activation of HER4 by heparin-binding EGF-like growth factor stimulates chemotaxis but not proliferation. EMBO J 1997;16:1268–78.
43. Clark RA. Biology of dermal wound repair. Dermatol Clin 1993;11:647–66.
44. Marikovsky M, Breuing K, Liu PY, et al. Appearance of heparin-binding EGF-like growth factor in wound fluid as a response to injury. Proc Natl Acad Sci USA 1993;90:3889–93.
45. Tokumaru S, Higashiyama S, Endo T, et al. Ectodomain shedding of epidermal growth factor receptor ligands is required for keratinocyte migration in cutaneous wound healing. J Cell Biol 2000;151:209–20.
46. Iwamoto R, Handa K, Mekada E. Contact-dependent growth inhibition and apoptosis of epidermal growth factor (EGF) receptor-expressing cells by the membrane-anchored form of heparin-binding EGF-like growth factor. J Biol Chem 1999;274: 25906–12.
47. Gangarosa LM, Sizemore N, Graves-Deal R, Oldham SM, Der CJ, Coffey RJ. A raf-independent epidermal growth factor receptor autocrine loop is necessary for Ras transformation of rat intestinal epithelial cells. J Biol Chem 1997;272:18926–31.
48. Plate KH, Breier G, Weich HA, Risau W. Vascular endothelial growth factor is a potential tumour angiogenesis factor in human gliomas *in vivo*. Nature (Lond.) 1992;359:845–8.
49. Wells A. EGF receptor. Int J Biochem. Cell Biol 1999;31:637–43.
50. Hiratsuka S, Nakamura K, Iwai S, et al. MMP9 induction by vascular endothelial growth factor receptor-1 is involved in lung-specific metastasis. Cancer Cell 2002; 2:289–300.

Article

Distinct roles for ADAM10 and ADAM17 in ectodomain shedding of six EGFR ligands

Umut Sahin,[1,2] Gisela Weskamp,[1] Kristine Kelly,[1,3] Hong-Ming Zhou,[1] Shigeki Higashiyama,[4] Jacques Peschon,[5] Dieter Hartmann,[6] Paul Saftig,[7] and Carl P. Blobel[1]

[1]Cell Biology Program, Sloan-Kettering Institute, Memorial Sloan-Kettering Cancer Center, New York, NY 10021
[2]Department of Molecular and Cellular Biology and Biochemistry, Brown University, Providence, RI 02912
[3]Weill Graduate School of Medical Sciences of Cornell University, New York, NY 10021
[4]Department of Medical Biochemistry, Ehime University School of Medicine, Ehime 791-0301, Japan
[5]Amgen Inc., Seattle, WA 98101
[6]Department for Human Genetics, K.U. Leuven and Flanders Interuniversity Institute for Biotechnology (VIB-4), 3000 Leuven, Belgium
[7]Biochemical Institute, Christian-Albrechts University, D-24098 Kiel, Germany

All ligands of the epidermal growth factor receptor (EGFR), which has important roles in development and disease, are released from the membrane by proteases. In several instances, ectodomain release is critical for activation of EGFR ligands, highlighting the importance of identifying EGFR ligand sheddases. Here, we uncovered the sheddases for six EGFR ligands using mouse embryonic cells lacking candidate-releasing enzymes (a disintegrin and metalloprotease [ADAM] 9, 10, 12, 15, 17, and 19). ADAM10 emerged as the main sheddase of EGF and betacellulin, and ADAM17 as the major convertase of epiregulin, transforming growth factor α, amphiregulin, and heparin-binding EGF-like growth factor in these cells. Analysis of *adam9/12/15/17*$^{-/-}$ knockout mice corroborated the essential role of *adam17*$^{-/-}$ in activating the EGFR in vivo. This comprehensive evaluation of EGFR ligand shedding in a defined experimental system demonstrates that ADAMs have critical roles in releasing all EGFR ligands tested here. Identification of EGFR ligand sheddases is a crucial step toward understanding the mechanism underlying ectodomain release, and has implications for designing novel inhibitors of EGFR-dependent tumors.

Introduction

The epidermal growth factor receptor (EGFR) signaling pathway has critical functions in development and in diseases such as cancer (Yarden and Sliwkowski, 2001). Ligands of the EGFR comprise a family of structurally and functionally related integral membrane proteins that can be proteolytically processed and released from cells (Harris et al., 2003). EGFR ligands include EGF (Cohen, 1965), heparin-binding EGF-like growth factor (HB-EGF; Higashiyama et al., 1991), TGFα (Derynck et al., 1984), betacellulin (Shing et al., 1993), amphiregulin (Shoyab et al., 1989), epiregulin (Toyoda et al., 1995), and epigen (Strachan et al., 2001). Although membrane-bound EGFR ligands can engage in juxtacrine signaling (Brachmann et al., 1989; Wong et al., 1989; Higashiyama et al., 1991), a metalloprotease activity is critical for activation of EGFR signaling under a variety of circumstances. For example, EGFR-dependent proliferation and migration of a mammary epithelial cell line can be inhibited by the metalloprotease inhibitor batimastat (BB94), and this inhibition is rescued by addition of soluble EGF (Dong et al., 1999). Furthermore, activation of TGFα and potentially other EGFR ligands during mouse development depends on the presence of functional ADAM17 (Peschon et al., 1998). Moreover, the metalloprotease-dependent release of HB-EGF as well as amphiregulin from cells has been described as a key step in the transactivation of the EGFR by different G protein–coupled receptors (GPCRs; Prenzel et al., 1999; Gschwind et al., 2003; Lemjabbar et al., 2003). Production

Address correspondence to Carl P. Blobel, Cell Biology Program, Sloan-Kettering Institute, Memorial Sloan-Kettering Cancer Center, Box 368, 1275 York Avenue, New York, NY 10021. Tel.: (212) 639-2915. Fax: (212) 717-3047. email: c-blobel@ski.mskcc.org

Key words: EGF receptor; EGF receptor ligands; ADAMs; ectodomain shedding; growth factor signaling

Abbreviations used in this paper: ADAM, a disintegrin and metalloprotease; AP, alkaline phosphatase; EGFR, epidermal growth factor receptor; GPCR, G protein–coupled receptor; HB-EGF, heparin-binding EGF-like growth factor; MEF, mouse embryonic fibroblast; TACE, TNFα-converting enzyme.

Table I. **Genotype of offspring from matings of *adam9*$^{+/-}$*15*$^{+/-}$ parents**

Genotype of offspring	Expected	Observed
	%	%
$9^{+/+}15^{+/+}$	6.25	5.5 (10)
$9^{+/+}15^{+/-}$	12.5	15.0 (27)
$9^{+/+}15^{-/-}$	6.25	5.0 (9)
$9^{+/-}15^{+/+}$	12.5	12.8 (23)
$9^{+/-}15^{+/-}$	25.0	23.9 (43)
$9^{+/-}15^{-/-}$	12.5	12.8 (23)
$9^{-/-}15^{+/+}$	6.25	5.5 (10)
$9^{-/-}15^{+/-}$	12.5	15.5 (27)
$9^{-/-}15^{-/-}$	6.25	4.4 (8)

Numbers in parentheses, # (total of 180).

Table II. **Genotype of offspring from matings of *adam9*$^{-/-}$*15*$^{-/-}$*12*$^{+/-}$ parents**

Genotype of offspring	Percent
$9^{-/-}15^{-/-}12^{+/+}$	30.1 (50)
$9^{-/-}15^{-/-}12^{+/-}$	44.0 (73)
$9^{-/-}15^{-/-}12^{-/-}$	25.9 (43)

Numbers in parentheses, # (total of 166).

of soluble HB-EGF by keratinocytes is up-regulated in response to wounding, and a metalloprotease inhibitor that blocks release of EGFR ligands from these cells abolishes their migration in vitro, and wound healing in vivo (Tokumaru et al., 2000). Shedding of HB-EGF also has an important role in heart development (Jackson et al., 2003; Yamazaki et al., 2003) and in a mouse model of myocardial hypertrophy, which can be prevented through a metalloprotease inhibitor (Asakura et al., 2002). A recent report demonstrates that even juxtacrine activation of the EGFR by TGFα on an adjacent cell can require a metalloprotease activity (Borrell-Pages et al., 2003). Finally, all three EGFR ligands in *Drosophila* (Spitz, Gurken, and Keren) are activated via cleavage of their transmembrane anchors (Lee et al., 2001; Urban et al., 2001; Ghiglione et al., 2002; Tsruya et al., 2002; Shilo, 2003). However, in *Drosophila*, different proteolytic enzymes, the Rhomboid-type proteases, have been implicated in this process (Urban et al., 2002). Thus, proteolytic processing of EGFR ligands is emerging as a critical step in their functional regulation under several different circumstances.

Metalloproteases of the ADAM (a disintegrin and metalloprotease) family are thought to be responsible for shedding of certain EGFR ligands. ADAMs are membrane-anchored glycoproteins with diverse functions, including critical roles in fertilization, neurogenesis, angiogenesis, and in shedding of membrane-bound proteins from cells (Black and White, 1998; Schlöndorff and Blobel, 1999; Primakoff and Myles, 2000; Seals and Courtneidge, 2003). Mice lacking ADAM17 die perinatally and resemble mice lacking TGFα (Mann et al., 1993), HB-EGF (Iwamoto et al., 2003; Jackson et al., 2003), and the EGFR (Miettinen et al., 1995; Sibilia and Wagner, 1995; Threadgill et al., 1995; Peschon et al., 1998). Consistent with these observations, ADAM17-deficient cells have been shown to be defective in shedding of TGFα, HB-EGF, and amphiregulin (Peschon et al., 1998; Merlos-Suarez et al., 2001; Sunnarborg et al., 2002). However, in addition to ADAM17, three other ADAMs have been linked to HB-EGF shedding. Overexpression of ADAM9 increases HB-EGF shedding in VeroH cells, whereas a mutant form of ADAM9 that is presumably unfolded and retained in the ER decreases HB-EGF shedding (Izumi et al., 1998); yet no defect in HB-EGF shedding was observed in cells lacking ADAM9 (Weskamp et al., 2002). Furthermore, ADAM12 reportedly has a role in HB-EGF shedding in the heart (Asakura et al., 2002) and in the down-regulation of cell-associated HB-EGF after stimulation with the phorbol ester PMA (Kurisaki et al., 2003). ADAM10 is the fourth ADAM to be implicated in HB-EGF shedding as part of the crosstalk between GPCRs and the EGFR (Lemjabbar and Basbaum, 2002; Yan et al., 2002). The remaining EGFR ligands, EGF, betacellulin, epiregulin, and epigen, are also known to be shed from cells, yet little information is available about the responsible enzyme(s) (Dempsey et al., 1997; Harris et al., 2003).

A crucial step toward understanding the mechanism underlying proteolytic cleavage of EGFR ligands (and its potential role in their activation) is to identify the responsible enzyme(s). In previous papers, different cell types and different approaches were used to analyze shedding of some EGFR ligands (see previous paragraphs), including antisense oligonucleotides and overexpression of both wild-type and putative dominant-negative ADAM constructs. Here, we chose a genetically defined system that is less prone to potential artifacts to evaluate the role of ADAMs in EGFR ligand shedding. To address potential compensatory or redundant functions between ADAMs 9, 12, 15, and 17, we generated *adam9/12/15*$^{-/-}$ and *adam9/12/15/17*$^{-/-}$ mice. Furthermore, we used cells isolated from wild-type, *adam9/12/15*$^{-/-}$, *adam10*$^{-/-}$, *adam17*$^{-/-}$, *adam19*$^{-/-}$, or *adam9/12/15/17*$^{-/-}$ mice to evaluate how loss of one or more widely expressed ADAMs affects the shedding of different EGFR ligands. This paper represents the first systematic characterization of EGFR ligand processing using mouse cells that lack one or more candidate sheddase of the ADAM family of metalloproteases.

Results

Generation of *adam9/12/15*$^{-/-}$ triple knockout mice to assess potential compensatory or redundant roles of these candidate EGFR ligand sheddases in mouse development

ADAMs 9 and 12 have previously been implicated as sheddases for HB-EGF (Izumi et al., 1998; Asakura et al., 2002; Kurisaki et al., 2003). To evaluate potential redundant or compensatory roles of ADAMs 9 and 12, as well as the related ADAM 15 in development and in the shedding of HB-EGF and other EGFR ligands, we generated double knockout mice (*adam9/15*$^{-/-}$) and triple knockout mice (*adam9/12/15*$^{-/-}$) as described in the Materials and methods. Table I shows that *adam9/15*$^{-/-}$ double knockout mice were born with the expected Mendelian ratio from matings of doubly heterozygous parents. *adam9/15*$^{-/-}$ mice were viable and fertile, and did not display any evident spontaneous pathological phenotypes (see Materials and methods for details).

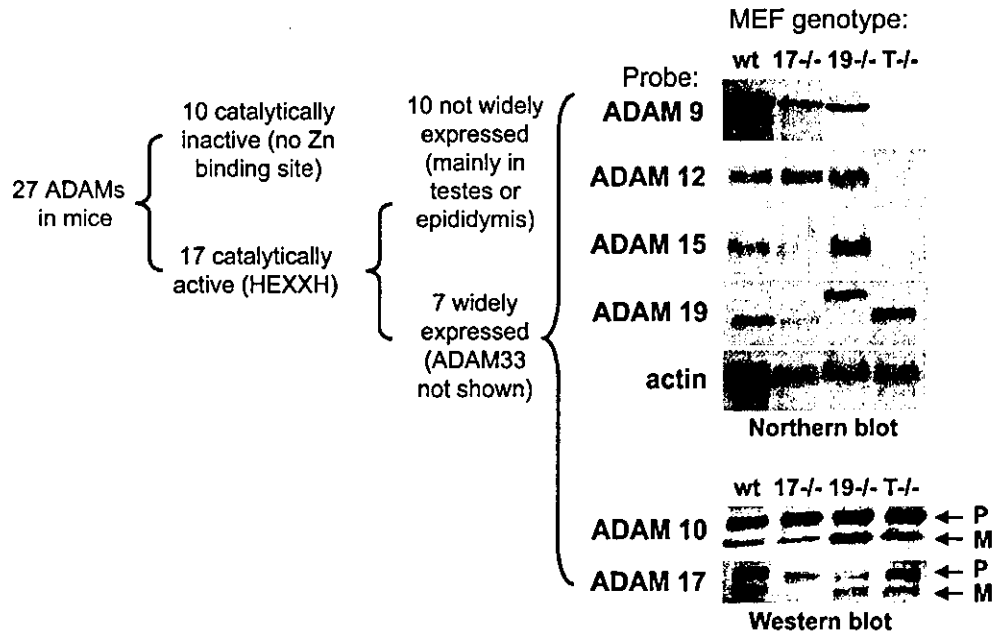

Figure 1. **Expression of widely expressed and catalytically active ADAMs in MEFs.** ADAMs are grouped by expression pattern and presence or absence of a catalytic site (HEXXH) in the metalloprotease domain. 27 ADAMs have been identified in mice, of which 10 lack an HEXXH sequence, and are presumably not catalytically active. Out of 17 ADAMs with an HEXXH sequence, 10 are mainly expressed in the testes or epididymis, or are not widely expressed (J.M. White, University of Virginia, Charlottesville, VA; http://www.people.virginia.edu/%7Ejw7g/Table_of_the_ADAMs.html). Six of the seven widely expressed HEXXH-containing ADAMs were included in this paper. The top right panel shows a Northern blot analysis of the expression of ADAMs 9, 12, 15, and 19 in primary MEFs. The ADAM19 mRNA in *adam19*$^{-/-}$ cells is larger than in the other cells analyzed because the ADAM19 gene is disrupted by insertion of a secretory gene trap (Zhou et al., 2004). The bottom right panel is a Western blot depicting expression of ADAMs 10 and 17 in the primary embryonic fibroblasts used here. Both pro- and mature ADAM10 are expressed in all primary mEFs analyzed here, and pro- and mature ADAM17 are expressed in wild-type, *adam19*$^{-/-}$, and *adam9/12/15*$^{-/-}$ cells. Note that the exon containing the Zn^{2+}-binding catalytic site of ADAM17 is deleted in *adam17*$^{-/-}$ cells (ADAM17$^{\Delta Zn/\Delta Zn}$). This will most likely impair proper protein folding, resulting in retention of mutant ADAM17 in the ER by chaperones and subsequent degradation (Suzuki et al., 1998). wt, wild type; 17$^{-/-}$, *adam17*$^{-/-}$; 19$^{-/-}$, *adam19*$^{-/-}$; T$^{-/-}$, *adam9/12/15*$^{-/-}$ triple knockout; P, pro-form; M, mature.

Triple knockout mice lacking ADAMs 9, 12, and 15 were generated by mating *adam9/15*$^{-/-}$ parents carrying one mutant ADAM12 allele (*adam9/15*$^{-/-}$*12*$^{+/-}$). The genotype of offspring from these matings was Mendelian with respect to the mutant ADAM12 allele (Table II), and *adam9/12/15*$^{-/-}$ triple knockout mice were viable and fertile and did not display any evident pathological phenotypes (see below, and Materials and methods for details).

Ectodomain shedding of EGFR ligands in mouse embryonic fibroblasts

To further explore the role of ADAMs in EGFR ligand shedding, we turned to cell-based assays using cells isolated from triple knockout *adam9/12/15*$^{-/-}$ mice, as well as from animals lacking ADAM10, ADAM17, or ADAM19, and wild-type controls. This allowed us to evaluate the contribution of all but one of the widely expressed and catalytically active ADAMs (ADAMs 9, 10, 12, 15, 17, and 19; see Fig. 1; ADAM33 was not included in this work) to the shedding of the EGFR ligands TGFα, amphiregulin, epiregulin, HB-EGF, betacellulin, and EGF. The general approach was to transfect cells with alkaline phosphatase (AP)–tagged forms of EGFR ligands, and then to quantitate shedding by measuring AP activity released into the culture supernatant, or by an in-gel detection of the released AP domain (Weskamp et al., 2002; Zheng et al., 2002; see Materials and methods for details). Because immortalization of primary cells can significantly affect the expression pattern of ADAMs and other genes (unpublished data), shedding experiments were performed with primary E13.5 mouse embryonic fibroblasts (MEFs) whenever this was possible. The only exceptions were *adam10*$^{-/-}$ and *adam10*$^{+/-}$ cell lines, which were immortalized because *adam10*$^{-/-}$ embryos die early in embryogenesis (E9.5) (Hartmann et al., 2002). Northern or Western blot analyses confirmed that primary mEFs from wild-type mice indeed express all ADAMs analyzed here (ADAMs9, 10, 12, 15, 17, and 19; see Fig. 1). Furthermore, Northern blots of RNA isolated from primary *adam*$^{-/-}$ cells confirmed the absence of wild-type RNA for the corresponding targeted ADAM(s). Finally, Western blot analysis confirmed that ADAM10 is expressed in all *adam*$^{-/-}$ primary mEFs, and that no mature ADAM17 is produced in *adam17*$^{-/-}$ cells.

As differences in expression levels between tissue culture wells or separate experiments might affect the interpretation of these experiments, each data point was derived from two consecutive measurements of AP activity shed from a single transfected well (see Fig. 2 A). Stimulation of EGFR ligand shedding in a given well was determined by collecting medium after 1 h from unstimulated cells, and then after 1 h from the same cells stimulated with the phorbol ester PMA, a

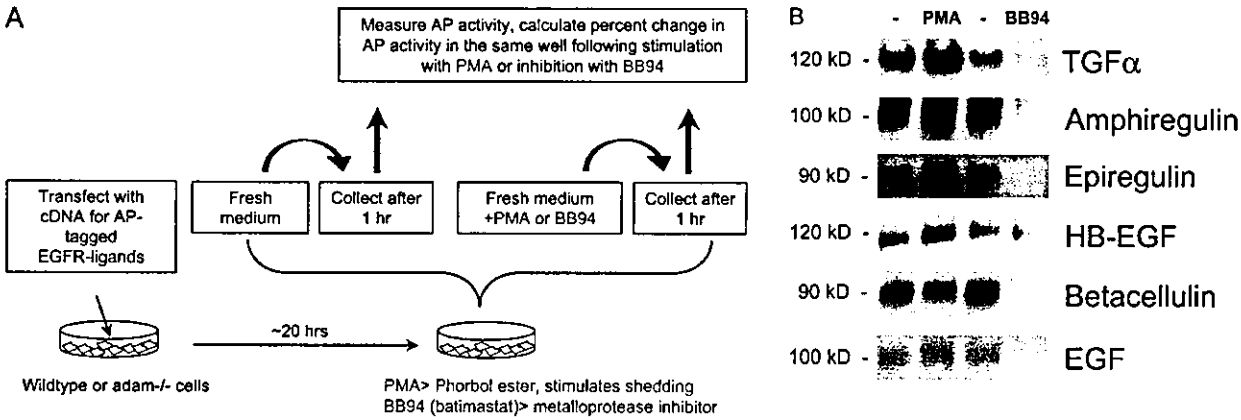

Figure 2. **Shedding of EGFR ligands in wild-type primary MEFs.** (A) Diagram of a typical shedding experiment (see text for details). (B) Detection of shed AP-tagged EGFR ligands after renaturation in SDS gels (see Materials and methods for details). The left lane shows the AP-tagged forms of TGFα, amphiregulin, epiregulin, HB-EGF, betacellulin, and EGF released in 1 h into the supernatant of a single well each of transfected mEF under resting conditions. The next lane shows the EGFR ligands released in 1 h from the same well after addition of PMA, a phorbol ester that stimulates ectodomain shedding. The third lane shows EGFR ligands released from a separate well in 1 h under resting conditions, and the fourth lane shows the released EGFR ligands in that same well after addition of the hydroxamate-based metalloprotease inhibitor batimastat (BB94).

commonly used activator of ectodomain shedding (Massague and Pandiella, 1993; Hooper et al., 1997; see Fig. 3 A). This was used to calculate the increase in shedding in a given well during PMA stimulation. The batimastat-sensitive constitutive shedding was determined similarly, by measuring the decrease in AP activity in media collected after 1 h in the presence of batimastat and comparing it to the AP activity released from the same well collected 1 h before treatment (see Fig. 4 A). This single-well assay minimizes possible effects caused by different transfection levels. Nevertheless, the absolute values for constitutive shedding from different wild-type or primary *adam*$^{-/-}$ cells expressing a given EGFR ligand were also determined to provide a reference point for the comparison of total unstimulated shedding levels.

Shedding of EGFR ligands in wild-type cells

Shedding of EGFR ligands was first evaluated in wild-type MEFs. As shown in Fig. 2 B, unstimulated mEFs shed basal amounts of TGFα, amphiregulin, epiregulin, HB-EGF, betacellulin, and EGF. In the case of TGFα, amphiregulin, epiregulin, and HB-EGF, shedding was stimulated relatively strongly by PMA, whereas shedding of betacellulin and EGF was only weakly enhanced by PMA (see also Fig. 3 A). Treatment with the metalloprotease inhibitor batimastat strongly reduced both PMA-stimulated (unpublished data) and constitutive shedding of all EGF family members except HB-EGF. Although stimulated HB-EGF shedding was effectively inhibited by batimastat (unpublished data), constitutive release was only weakly affected (see also Fig. 4 A), suggesting that the predominant constitutive HB-EGF sheddase in primary mEFs is not a batimastat-sensitive metalloprotease, and is distinct from the sheddase(s) of other EGFR ligands.

PMA-stimulated shedding of EGFR ligands in *adam*$^{-/-}$ cells

The potential role of different ADAMs as EGFR ligand sheddases was then addressed in *adam*$^{-/-}$ mEFs. When we evaluated PMA-stimulated EGFR ligand shedding in triple knockout *adam9/12/15*$^{-/-}$ cells, no significant decrease in the release of HB-EGF, TGFα, amphiregulin, EGF, or betacellulin compared with wild-type cells was observed (Fig. 3 A). However, there was a statistically significant reduction in stimulated shedding of epiregulin in *adam9/12/15*$^{-/-}$ cells (41.8%), suggesting that one or more of these ADAMs contributes to stimulated epiregulin processing. Similarly, we found no evidence for a major role of ADAM19 in stimulated shedding of the EGFR ligands tested here (Fig. 3 A). The reason for the slight increase in HB-EGF shedding in *adam19*$^{-/-}$ cells compared with wild-type controls remains to be determined.

ADAM17 has been implicated in the shedding of TGFα and HB-EGF in immortalized embryonic fibroblasts and primary keratinocytes (Peschon et al., 1998; Merlos-Suarez et al., 2001; Sunnarborg et al., 2002), and of amphiregulin in primary keratinocytes (Sunnarborg et al., 2002). Consistent with these results, we observed a significant reduction of PMA-induced shedding of TGFα (89%), amphiregulin (65.8%), and HB-EGF (58.1%) in *adam17*$^{-/-}$ compared with wild-type mEFs (Fig. 3 A). Furthermore, shedding of epiregulin was also strongly decreased in *adam17*$^{-/-}$ cells (75.7%), providing the first evidence for a critical role of ADAM17 in stimulated shedding of this EGFR ligand. For TGFα, amphiregulin, and epiregulin, PMA-dependent ectodomain shedding in *adam17*$^{-/-}$ cells was increased when wild-type ADAM17 was cotransfected, confirming that the defect in PMA-dependent shedding is indeed due to loss of ADAM17 (unpublished data).

ADAM10 has been implicated in shedding of HB-EGF as part of a pathway for crosstalk between a GPCR and the EGFR (Lemjabbar and Basbaum, 2002; Yan et al., 2002). As shown in Fig. 3, PMA-stimulated shedding of HB-EGF, TGFα, amphiregulin, and epiregulin is not decreased in *adam10*$^{-/-}$ cells, suggesting that ADAM10 is not required for the PMA-stimulated shedding of these EGFR ligands. The enhanced stimulated shedding of these EGFR ligands

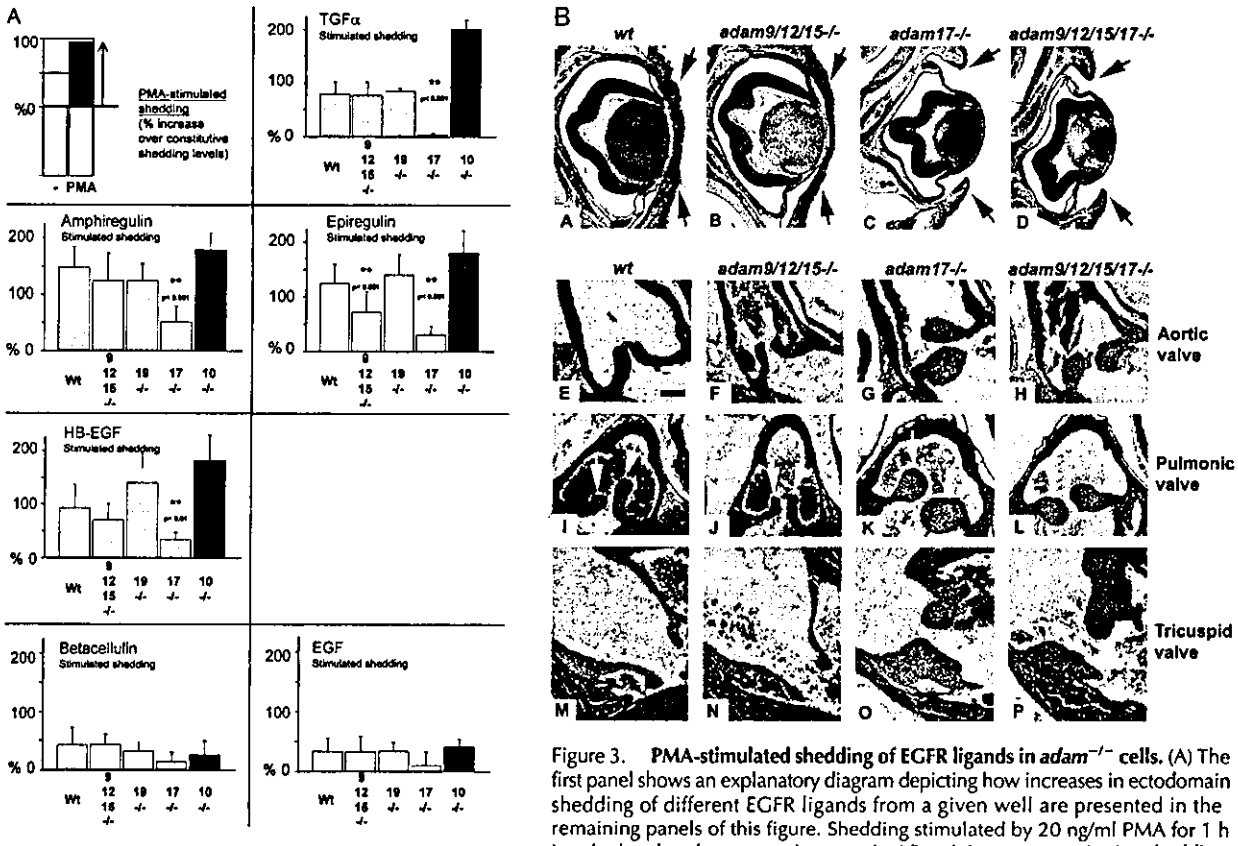

Figure 3. **PMA-stimulated shedding of EGFR ligands in *adam*$^{-/-}$ cells.** (A) The first panel shows an explanatory diagram depicting how increases in ectodomain shedding of different EGFR ligands from a given well are presented in the remaining panels of this figure. Shedding stimulated by 20 ng/ml PMA for 1 h is calculated as the percent increase in AP activity over constitutive shedding in the same well for 1 h. The next panels only show the PMA-dependent increase in shedding over constitutive levels for each EGFR ligand and each *adam*$^{-/-}$ cell type. Data from primary mEFs (yellow bars) are compiled from separate experiments using cells from three or more litters for each *adam*$^{-/-}$ mouse line. Only *adam10*$^{-/-}$ and control *adam10*$^{+/-}$ cells were immortalized (blue bars). Overall, at least four separate wells were evaluated per EGFR ligand. The results indicate that ADAM17 is the major stimulated sheddase for TGFα, amphiregulin, epiregulin, and HB-EGF. ADAMs 9, 12, or 15 (or a combination of two or more of these ADAMs) also contribute to stimulated epiregulin shedding. On the other hand, the shedding of betacellulin and EGF is only weakly stimulated by PMA. Because the increase in stimulated shedding is small, no statistically significant differences in stimulated shedding of betacellulin or EGF was seen in *adam*$^{-/-}$ cells compared with wild-type controls. (B) Histological analysis of sectioned hematoxylin and eosin–stained eyes and eyelids (A–D), aortic valves (E–H), pulmonic valves (I–L), and tricuspid valves (M–P) of newborn wild-type (A, E, I, and M), *adam9/12/15*$^{-/-}$ (B, F, J, and N), *adam17*$^{-/-}$ (C, G, K, and O), and *adam9/12/15/17*$^{-/-}$ (D, H, L, and P) mice. Eyelids of wild-type and *adam9/12/15*$^{-/-}$ mice are closed at birth (A and B), whereas those of *adam17*$^{-/-}$ and *adam9/12/15/17*$^{-/-}$ mice are open (C and D). The aortic, pulmonic, and tricuspid valves of *adam9/12/15*$^{-/-}$ mice (F, J, and N) resemble those of wild-type mice (E, I, and M, respectively), whereas these valves are thickened and misshapen in *adam17*$^{-/-}$ (G, K, and C) and *adam9/12/15/17*$^{-/-}$ quadruple knockout mice (H, L, and P). The valve defects in *adam9/12/15/17*$^{-/-}$ quadruple knockout mice, which also include thickened and misshapen mitral valves (not depicted), are comparable to those in *adam17*$^{-/-}$ mice. Eyelids in A–D marked by red arrows, heart valves in E–P marked by yellow arrows. Bar (E–P), 100 μm.

in *adam10*$^{-/-}$ (Fig. 3 A) and *adam10*$^{+/-}$ cells (unpublished data) compared with the primary mEFs is presumably a consequence of immortalization.

Generation of *adam9/12/15/17*$^{-/-}$ quadruple knockout mice, and evaluation of PMA-stimulated EGFR ligand shedding in *adam9/12/15/17*$^{-/-}$ cells

Although ADAM17 is essential for the majority of stimulated shedding of HB-EGF in mEF cells, a residual amount of PMA-stimulated HB-EGF shedding is seen in the absence of ADAM17. Could this residual shedding depend on ADAMs 9 or 12, both of which have been implicated in HB-EGF shedding, or on the related ADAM15? To address this issue, we generated quadruple knockout mice lacking ADAMs 9, 12, 15, and 17 (see Materials and methods for details). Similar to *adam17*$^{-/-}$ mice, *adam9/12/15/17*$^{-/-}$ quadruple knockout mice that were born had open eyes and died in the first day after birth. The percentage of *adam9/12/15/17*$^{-/-}$ quadruple knockout embryos at E18.5 generated by mating *adam9*$^{-/-}$*12*$^{-/-}$*15*$^{-/-}$*17*$^{+/-}$ parents was somewhat lower than the percentage of *adam17*$^{-/-}$ embryos at E17.5–18.5 produced by mating *adam17*$^{+/-}$ mice (Table III; Peschon et al., 1998).

To determine whether the loss of ADAMs 9, 12, and 15 exacerbates known defects in EGFR signaling in *adam17*$^{-/-}$ mice, we performed a histopathological examination of wild-type, *adam9/12/15*$^{-/-}$, *adam17*$^{-/-}$, and *adam9/12/15/17*$^{-/-}$ E18.5 embryos. As shown in Fig. 3 B (panels A–D), the open-eye phenotype in *adam17*$^{-/-}$ mice that results from lack of TGFα activation (Peschon et al., 1998) is similar in *adam9/*

Table III. **Offspring of matings of *adam9/12/15*$^{-/-}$*17*$^{+/-}$ parents**

Genotype of E18.5 embryos	Percent
$9^{-/-}15^{-/-}12^{-/-}17^{+/+}$	36.7 (36)
$9^{-/-}15^{-/-}12^{-/-}17^{+/-}$	49.0 (48)
$9^{-/-}15^{-/-}12^{-/-}17^{-/-}$	14.3 (14) [4]
Genotype of E17.5–18.5 embryos	
$17^{+/+}$	23.3 (23)
$17^{+/-}$	57.3 (59)
$17^{-/-}$	20.4 (21) [4]

Genotype of E18.5 embryos from matings of $adam9^{-/-}15^{-/-}12^{-/-}17^{+/-}$ parents. Numbers in parentheses, # (total of 98). Genotype of E17.5–18.5 embryos from matings of $adam17^{+/-}$ parents, taken from Peschon et al. (1998). Numbers in parentheses, # (total of 103). Nonviable embryos are indicated in brackets.

12/15/17$^{-/-}$ quadruple knockout mice, whereas it is not seen in *adam9/12/15*$^{-/-}$ triple knockout mice. Furthermore, Jackson et al. (2003) have described a defect in morphogenesis of the semilunar heart valves and the tricuspid and mitral valves in *adam17*$^{-/-}$ mice (Fig. 3 B, panels E–P; mitral valve not depicted), which resembles the thickened and misshapen valves seen in *hb-egf*$^{-/-}$ mice and in mice with a knock-in mutation that abolishes HB-EGF shedding (Iwamoto et al., 2003; Yamazaki et al., 2003). As shown in Fig. 3 B, the heart valves in *adam9/12/15*$^{-/-}$ triple knockout mice are indistinguishable from those in wild-type mice, and again, the defects in heart valve morphogenesis in *adam17*$^{-/-}$ mice are comparable to the defects in *adam9/12/15/17*$^{-/-}$ quadruple knockout mice. A morphometric analysis of all heart valves of six *adam9/12/15/17*$^{-/-}$ E18.5 embryos also did not show an increased size

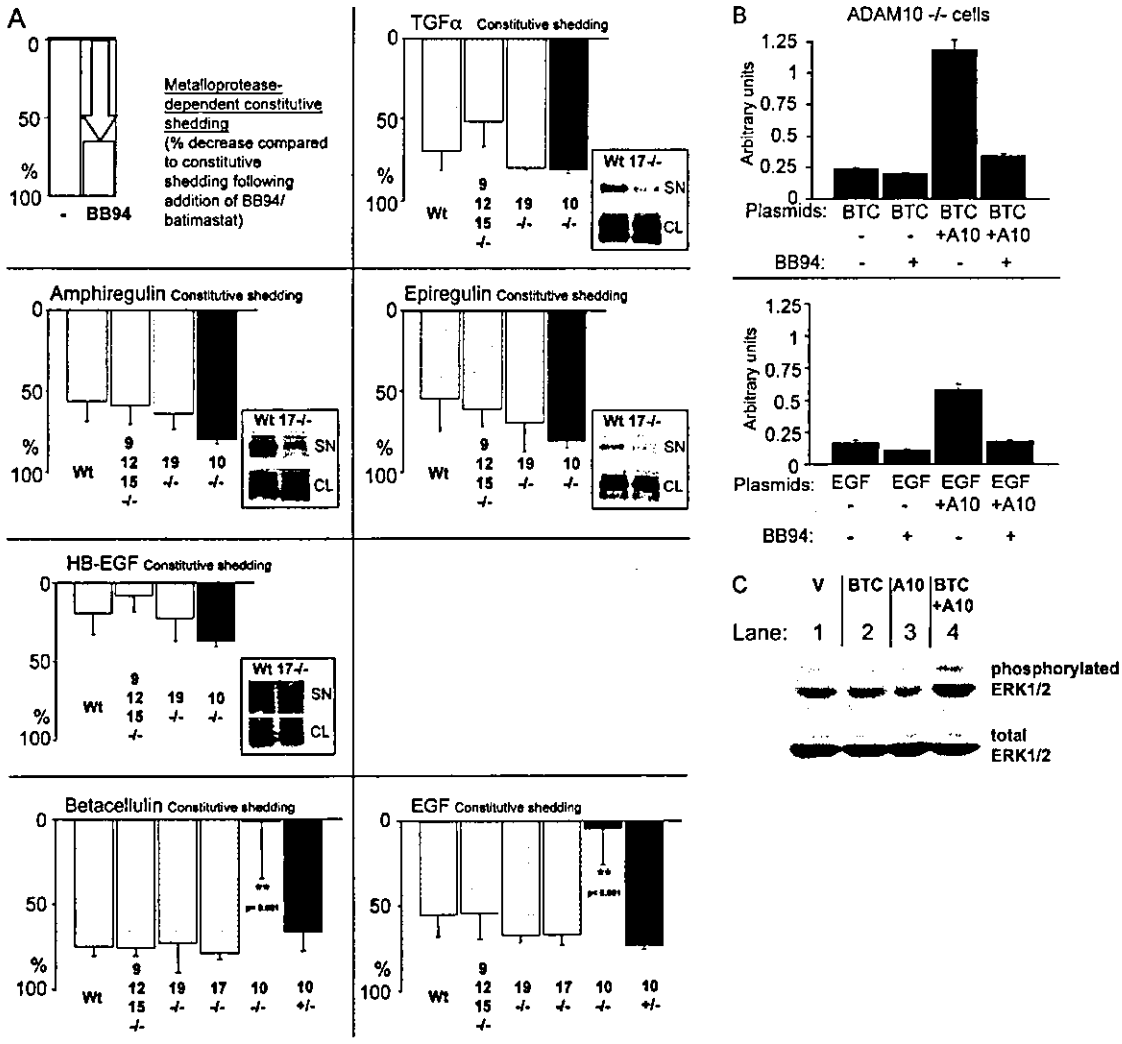

Figure 4. **Batimastat-sensitive constitutive shedding of EGFR ligands in *adam*$^{-/-}$ cells.** (A) A diagram indicating how the batimastat-sensitive component of ectodomain shedding of different EGFR ligands from a given well of resting cells was determined. Shedding of EGFR ligands in 1 h from resting cells is used as a reference to determine the percentage of batimastat-sensitive constitutive shedding (percent decrease after addition of batimastat). The next panels show the batimastat-sensitive decrease in shedding of each EGFR ligand in each *adam*$^{-/-}$ cell type. As in Fig. 3, separate experiments were performed with cells from three or more litters for each *adam*$^{-/-}$ mouse line. At least six separate wells were analyzed for *adam10*$^{-/-}$ and control *adam10*$^{+/-}$ cells, which were immortalized (blue bars). Several wells were evaluated in each experiment for each lot of cells and for each EGFR ligand. The results show that ADAMs 9, 10, 12, 15, and 19 are not essential for the batimastat-

compared with six *adam17*$^{-/-}$ E18.5 embryos (unpublished data). When we performed shedding experiments with *adam9/12/15/17*$^{-/-}$ quadruple knockout mEFs, the residual amount of PMA-stimulated HB-EGF shedding was comparable to what is observed in *adam17*$^{-/-}$ cells (percent increase in HB-EGF shedding after PMA stimulation in *adam9/12/15/17*$^{-/-}$ mEF: 33.3 ± 26.5%, $n = 16$; four embryos, 2–6 wells analyzed per embryo); compared with 33.7 ± 12.9% in *adam17*$^{-/-}$ mEF; Fig. 3 A). Together, these results argue against a significant contribution of ADAMs 9, 12, or 15 to the shedding of HB-EGF in these cells.

Constitutive shedding of EGFR ligands in *adam*$^{-/-}$ cells

Next, we evaluated the batimastat-sensitive component of constitutive shedding of EGFR ligands in the presence or absence of different ADAMs. No significant difference in the batimastat-sensitive constitutive shedding of all six ligands tested here was observed in *adam9/12/15*$^{-/-}$ or *adam19*$^{-/-}$ cells compared with wild-type controls (Fig. 4 A). Furthermore, constitutive shedding of TGFα, amphiregulin, epiregulin, and HB-EGF was also not affected in *adam10*$^{-/-}$ cells.

Because the shedding assay used here relies on measurements of the percent increase (see above) or decrease in shedding after treatment compared with unstimulated shedding, it is important to ensure that the levels of unstimulated shedding are indeed similar in different *adam*$^{-/-}$ and wild-type cells. In experiments where wild-type cells were evaluated simultaneously with *adam9/12/15*$^{-/-}$ or *adam19*$^{-/-}$ cells, comparable amounts of each EGFR ligand analyzed here were released from unstimulated cells (unpublished data). However, the overall levels of constitutive shedding for TGFα, amphiregulin, epiregulin, and HB-EGF (but not EGF and betacellulin) were reduced in *adam17*$^{-/-}$ cells compared with wild-type controls (Fig. 4 A, insets; unpublished data). This demonstrates that ADAM17 has a key role in both stimulated and constitutive shedding of these EGFR ligands.

Interestingly, when we measured the batimastat-sensitive constitutive shedding of EGF and betacellulin, we found that it was abrogated in two independent *adam10*$^{-/-}$ cell lines compared with control *adam10*$^{+/-}$ cells and the primary mEF cells (Fig. 4 A; unpublished data). This resulted in a strong decrease in overall unstimulated constitutive shedding of betacellulin (87.5%) and EGF (49.7%) from *adam10*$^{-/-}$ cells compared with *adam10*$^{+/-}$ cells (unpublished data). Constitutive shedding of betacellulin and EGF could be rescued with wild-type ADAM10, confirming that the defect in shedding in *adam10*$^{-/-}$ cells is indeed due to the lack of ADAM10 (Fig. 4 B). Next, we evaluated the role of ADAM10 in betacellulin-dependent EGFR signaling in *adam10*$^{-/-}$ cells. When either ADAM10 or betacellulin were introduced in *adam10*$^{-/-}$ cells, there was no increase in phosphorylation of ERK1/2, a commonly used indicator for activation of the EGFR (Fig. 4 C). However, when wild-type ADAM10 was cotransfected with betacellulin in *adam10*$^{-/-}$ cells, ERK1/2 phosphorylation was increased (Fig. 4 C). Thus, EGFR signaling via transfected betacellulin depends on the presence of functional ADAM10 in these cells. Together, these results are the first to identify the major sheddase for EGF and betacellulin in mouse embryonic cells, and thus also to uncover two novel substrates for ADAM10.

To address whether the results obtained in mEF cells could in principle also be relevant for other cells and tissues, Western blot analysis of the expression of ADAMs 10 and 17 in different mouse tissues was performed (Fig. 5). This

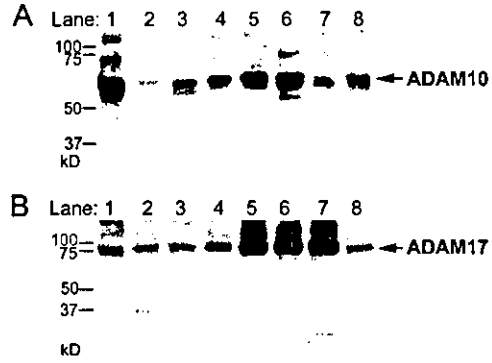

Figure 5. **Evaluation of ADAM10 and ADAM17 protein levels in different mouse tissues.** Western blots of mouse tissue extracts were probed with a polyclonal antiserum against ADAM10 (A) or ADAM17 (B). Equal amounts of Con A–enriched glycoproteins from the following tissues were loaded per lane: brain (lane 1), skeletal muscle (lane 2), kidney (lane 3), heart (lane 4), lung (lane 5), spleen (lane 6), testis (lane 7), and liver (lane 8). The arrow indicates the position of ADAM10 in A, and of ADAM17 in B.

sensitive constitutive shedding of TGFα, amphiregulin, epiregulin, and HB-EGF. The absolute levels of constitutive release of each EGFR ligand were comparable between wild-type, *adam9/12/15*$^{-/-}$, and *adam19*$^{-/-}$ cells (not depicted). However, the levels of constitutive shedding of TGFα, amphiregulin, epiregulin, and HB-EGF were significantly reduced in *adam17*$^{-/-}$ cells compared with wild-type controls (see inset gel figures; SN, supernatant; CL, cell lysate), indicating that ADAM17 is also the major constitutive sheddase for these ligands. Data on the batimastat-sensitive shedding in *adam17*$^{-/-}$ cells are not included in the graph because addition of batimastat further decreases the small amount of constitutive shedding in *adam17*$^{-/-}$ cells. Thus, another metalloprotease besides ADAM17 apparently makes a very minor contribution to shedding of these four substrates. The batimastat-sensitive shedding of betacellulin and EGF was very similar in *adam9/12/15*$^{-/-}$, *adam19*$^{-/-}$, *adam17*$^{-/-}$, and *adam10*$^{+/-}$ mEFs compared with wild-type controls. Although the absolute levels of constitutive shedding from these cells were also very similar (not depicted), constitutive shedding of betacellulin from *adam10*$^{-/-}$ cells was decreased by 87.5%, whereas shedding of EGF was decreased by 49.7% compared with *adam10*$^{+/-}$ cells. In the absence of ADAM10, the remaining small amount of constitutive shedding was not inhibitable by batimastat. (B) Batimastat-sensitive shedding of betacellulin (BTC) and EGF from *adam10*$^{-/-}$ cells can be rescued by cotransfection with wild-type ADAM10 (A10; each bar represents the results from six tissue culture wells). These results confirm that the defect in EGF and betacellulin shedding in *adam10*$^{-/-}$ cells is indeed due to the absence of ADAM10. (C) Constitutive phosphorylation of ERK1/2 in *adam10*$^{-/-}$ cells transfected with the pcDNA3 vector (V, lane 1) is not increased by transfection with BTC (lane 2) or ADAM10 (lane 3). However, ERK1/2 phosphorylation is increased when BTC and ADAM10 are cotransfected (lane 4), demonstrating that ADAM10 is critical for BTC-dependent EGFR signaling in these cells. The bottom panel shows the same blot reprobed with antibodies against total ERK1/2 to confirm equal loading in all lanes.

confirmed that both ADAMs are widely expressed, even though their expression levels vary. Thus, it is likely that both ADAMs 10 and 17 are expressed in the cells and tissues in which the ligands analyzed in this paper exert their function as activators of EGFR signaling.

Discussion

Protein ectodomain shedding of EGFR ligands can be critical for their functional activation. All EGFR ligands analyzed in this paper are synthesized as membrane-anchored precursors, and were initially identified as soluble biologically active growth factors (Cohen, 1962, 1965; de Larco and Todaro, 1978; Todaro et al., 1980; Shoyab et al., 1989; Higashiyama et al., 1991; Shing et al., 1993; Toyoda et al., 1995). A key step in elucidating the mechanism underlying the proteolytic release of EGFR ligands is the identification of the responsible sheddases. Although ADAM17 has been implicated in the shedding of TGFα, HB-EGF, and amphiregulin (Merlos-Suarez et al., 2001; Sunnarborg et al., 2002; Jackson et al., 2003), no information was previously available about the identity of the sheddases for epiregulin, EGF, and betacellulin. Furthermore, three other ADAMs (9, 10, and 12) had been implicated in HB-EGF shedding (Izumi et al., 1998; Asakura et al., 2002; Lemjabbar and Basbaum, 2002), raising questions about their individual contributions to HB-EGF release. To test the hypothesis that the sheddases for epiregulin, EGF, and betacellulin are also ADAMs, and to further evaluate the contribution of different ADAMs to HB-EGF shedding, we studied the release of these proteins from cells lacking one or more members of this family of metalloproteases. Moreover, even though ADAM17 has been linked to the shedding of TGFα and amphiregulin, we included these EGFR ligands in our paper both to investigate whether other ADAMs may participate in the shedding of these two proteins and as a positive control to validate the assay used here. Finally, we determined the effects of targeted deletions of up to four ADAMs that are candidate sheddases (ADAMs 9, 12, 15, and 17) on mouse development.

Ectodomain shedding experiments using these six major EGFR ligands in *adam*$^{-/-}$ MEFs corroborated previous reports that ADAM17 has a major role in the shedding of TGFα, HB-EGF, and amphiregulin (Peschon et al., 1998; Merlos-Suarez et al., 2001; Sunnarborg et al., 2002). We found no evidence for a major contribution of other ADAMs besides ADAM17 to TGFα, HB-EGF, and amphiregulin shedding in these cells. Furthermore, epiregulin was identified as a novel ADAM17 substrate. Previous works have shown that *adam17*$^{-/-}$ mice resemble *tgfα*$^{-/-}$ mice (Peschon et al., 1998) in that they have open eyes at birth, as well as displaying similar vibrissae, hair, and skin defects (Mann et al., 1993). Furthermore, *adam17*$^{-/-}$ mice also resemble *hb-egf*$^{-/-}$ mice (Iwamoto et al., 2003) in that they have thickened aortic and pulmonic valves (Jackson et al., 2003). A similar phenotype is seen in mice with a mutation in the cleavage site of HB-EGF that abolishes its shedding (Yamazaki et al., 2003). Finally, the phenotype of *adam17*$^{-/-}$ mice resembles that of *egfr*$^{-/-}$ mice (Miettinen et al., 1995; Sibilia and Wagner, 1995; Threadgill et al., 1995; Peschon et al., 1998). Thus, genetic experiments have substantiated that ADAM17 is also essential for the activation of EGFR ligands in vivo. It remains to be determined whether the lack of processing of amphiregulin or epiregulin (or both) also contributes to the phenotype of *adam17*$^{-/-}$ mice.

ADAMs 9, 10, and 12 are also considered candidate HB-EGF sheddases (Izumi et al., 1998; Asakura et al., 2002; Kurisaki et al., 2003). However, although PMA-stimulated ectodomain shedding of HB-EGF was somewhat reduced in *adam9/12/15*$^{-/-}$ cells, this reduction was not statistically significant. In addition, the residual PMA stimulation of HB-EGF shedding in *adam17*$^{-/-}$ cells is most likely also not due to ADAMs 9, 12, or 15 because it remains unchanged in *adam9/12/15/17*$^{-/-}$ quadruple knockout cells. In a previous paper, Kurisaki et al. (2003) reported a significant reduction in the down-regulation of cell-associated HB-EGF in phorbol ester–stimulated *adam12*$^{-/-}$ cells compared with wild-type controls. This apparent discrepancy may be due to differences in cell preparation or experimental design. Nevertheless, the main conclusion from the side-by-side comparison of different *adam*$^{-/-}$ cells isolated and cultured under identical conditions in this paper is that ADAM17 is the predominant PMA-stimulated HB-EGF sheddase in primary mEF cells.

The conclusion that ADAM17 has a critical role in shedding HB-EGF in vivo was further corroborated by an analysis of the role of these ADAMs during mouse development. As mentioned previously in this paper, *adam17*$^{-/-}$ mice resemble *egfr*$^{-/-}$, *tgfα*$^{-/-}$, or *hb-egf*$^{-/-}$ mice, whereas no similar defects were seen in *adam9/12/15*$^{-/-}$ mice. Furthermore, the phenotype of *adam17*$^{-/-}$ mice does not appear to be considerably exacerbated when ADAMs 9, 12, and 15 are also deleted. Together, these findings argue against major compensatory or redundant roles for ADAMs 9, 12, and the related ADAM 15 in the activation of TGFα, HB-EGF, or the EGFR during development. However, it cannot be ruled out that ADAMs 9, 12, or 15 contribute to shedding of EGFR ligands in cells or tissues where these enzymes and potential substrates are highly expressed. Further analyses will address which ADAMs are capable of cleaving EGFR ligands when overexpressed, and in which tissues candidate EGFR ligand sheddases besides ADAMs 10 and 17 are highly expressed together with EGFR ligands that they can cleave.

ADAM10 has also been implicated in HB-EGF shedding as part of a pathway that involves crosstalk between GPCRs and the EGFR (Lemjabbar and Basbaum, 2002; Yan et al., 2002; Lemjabbar et al., 2003). On the other hand, our results indicate that ADAM10 does not make a major contribution to PMA-stimulated or constitutive shedding of HB-EGF in the cells tested here. This is consistent with the notion that different stimuli may activate different ADAMs, such that HB-EGF shedding depends mainly on ADAM17 under the conditions used here, and mainly on ADAM10 when the appropriate GPCR is stimulated.

Little was previously known about the sheddases responsible for the release of EGF and betacellulin from cells. Here, we show that constitutive shedding of both EGF and betacellulin was strongly reduced in *adam10*$^{-/-}$ cells compared with heterozygous controls, and could be rescued by reintroduction of wild-type ADAM10. Furthermore, stimulation of the EGFR by transfected betacellulin in *adam10*$^{-/-}$ cells is only seen when these cells are rescued by cotransfection

with wild-type ADAM10. These results are the first to identify ADAM10 as the major sheddase for these two crucial EGFR ligands in mouse cells. Because ADAM10 is widely expressed, it is tempting to speculate that it may participate in the functional regulation of these two EGFR ligands in development and in diseases such as cancer.

In light of the genetic evidence for a key role of ADAM17 in activation of EGFR ligands in mice (Peschon et al., 1998; Sunnarborg et al., 2002; Jackson et al., 2003), it is surprising that no ADAM has been identified as an essential part of the EGFR pathway in *Drosophila* (Lee et al., 2001; Urban et al., 2001; Ghiglione et al., 2002; Tsruya et al., 2002; Shilo, 2003). Instead, Rhomboids (integral membrane proteins with seven membrane-spanning domains) have been implicated in cleaving EGFR ligands (Urban et al., 2002), whereas reducing the expression of a putative ADAM17 orthologue in *Drosophila* via small interfering RNA did not block development of EGFR-dependent structures (Lee et al., 2001).

These results suggest that there are critical differences in the mechanism underlying proteolytic activation of EGFR ligands between flies and mice. However, the finding that all EGFR ligands tested here are processed by ADAM10 or ADAM17 in mEFs suggests a possible alternative explanation for these findings. *Drosophila* carry orthologues of ADAM10 (KUZ) and ADAM17 (AAF56986, the ADAM targeted by RNA interference in Lee et al. [2001]), as well as a third ADAM related to ADAM17 and KUZ with no evident orthologue in mammals (AAF56926). It is conceivable that two or three of these ADAMs fulfill redundant or compensatory roles in activation of EGFR ligands during development in *Drosophila*. This may only become apparent once two or three of these putative EGFR ligand sheddases are simultaneously inactivated. Conversely, the results in *Drosophila* suggest that it will be worthwhile to further investigate the potential role of Rhomboids and intramembrane proteolysis in EGFR ligand activation in mammals.

In summary, we report the first systematic analysis of the shedding of EGFR ligands in cells lacking one or more widely expressed and catalytically active ADAM. Our results uncover critical roles for both ADAM10 and ADAM17 in shedding of EGFR ligands in mEF cells. ADAM17 emerged as the major PMA-stimulated and constitutive sheddase of TGFα, amphiregulin, HB-EGF, and epiregulin, which is consistent with the essential role for ADAM17 in activation of the EGFR during development. Furthermore, ADAM10 was found to be the major batimastat-sensitive sheddase for betacellulin and EGF in mEF. Further experiments, including the generation of conditional *adam10*$^{-/-}$ knockout mice, as well as knock-in mutations that abolish shedding of EGF and betacellulin, will be necessary to address the biological relevance of ADAM10 in shedding the endogenous forms of these EGFR ligands in vivo. The identification of different EGFR ligands as substrates for ADAM10 and ADAM17 sets the stage for the further analysis of how these ADAMs are regulated and how their substrate specificity is achieved. Because proteolysis of EGFR ligands may be critical for their functional activation, and signaling via the EGFR has been implicated in diseases such as cancer, ADAM10 and ADAM17 may be attractive targets for the design of drugs that modulate the action of these ligands.

Materials and methods

Generation of *adam9/15*$^{-/-}$, *adam9/12/15*$^{-/-}$, and *adam9/12/15/17*$^{-/-}$ knockout mice

Mice lacking ADAMs 9, 12, or 15 have been described previously (Weskamp et al., 2002; Horiuchi et al., 2003; Kurisaki et al., 2003). To generate *adam9/15*$^{-/-}$ double knockout mice, we mated *adam9*$^{+/-}$*15*$^{+/-}$ doubly heterozygous parents. This produced offspring in the expected Mendelian ratio (Table I). *adam9/15*$^{-/-}$ double knockout mice were then mated with *adam12*$^{-/-}$ mice (provided by Dr. Fujisawa-Sehara, University of Kyoto, Kyoto, Japan) to produce *adam9*$^{+/-}$*12*$^{+/-}$*15*$^{+/-}$ triple heterozygous parents. These were backcrossed with *adam9/15*$^{-/-}$ *mice* to generate *adam9/15* $^{/}$ *12*$^{+/}$ animals. When *adam9/15* $^{/}$ *12*$^{+/}$ mice were crossed, the ratio of offspring was Mendelian with respect to the mutant ADAM12 allele (Table II). Genotyping was performed by Southern blot as described previously (Weskamp et al., 2002; Horiuchi et al., 2003; Kurisaki et al., 2003). All animals used in this work were of mixed genetic background (129Sv/C57Bl6).

The histopathological analysis of *adam9/15*$^{-/-}$ mice was performed as described previously for *adam9*$^{-/-}$ or *adam15*$^{-/-}$ mice (Weskamp et al., 2002; Horiuchi et al., 2003). Histopathological analysis of *adam9/12/15* $^{-/}$ mice was performed by the Memorial Sloan-Kettering Cancer Center mouse phenotyping core. No abnormalities or pathological phenotypes were observed in *adam9/15*$^{-/-}$ and *adam9/12/15*$^{-/-}$ mice. Serial sections of tissues affected in *egfr*$^{-/-}$, *hb-egf*$^{-/-}$, and *tgfα*$^{-/-}$ mice did not uncover any evident defects in *adam9/12/15*$^{-/-}$ mice. Specifically, there were no defects in the development of the heart or its valves (Fig. 3 B, panels E–P), and also no defects in epithelia, intestine, lung, or in hair development. Finally, *adam9/12*$^{-/-}$ double knockout and *adam9/12/15*$^{-/-}$ triple knockout mice were indistinguishable from wild-type controls in their appearance and behavior during routine handling.

To generate *adam9/12/15/17*$^{-/-}$ quadruple knockout mice, *adam9/12/15*$^{-/-}$ triple knockout mice were mated with *adam17*$^{-/-}$ animals. Offspring from this mating that were heterozygous for the targeted allele of all four ADAMs were identified by Southern blotting, and were backcrossed several times with *adam9/12/15*$^{-/-}$ triple knockout mice to obtain *adam9*$^{-/-}$ *12*$^{-/-}$*15*$^{-/-}$*17*$^{+/-}$ mice. Crosses of *adam9*$^{-/-}$*12*$^{-/-}$*15*$^{-/-}$*17*$^{-/-}$ mice produced litters with a similar distribution of the targeted ADAM17 allele at E18.5 to what has been reported from crosses of *adam17*$^{+/-}$ mice (Table III; Peschon et al., 1998). Histopathological evaluation of newborn *adam9/12/15/17*$^{-/-}$ quadruple knockout mice did not uncover any significant worsening of the developmental defects described for *adam17*$^{-/-}$ mice. The cause for the slightly increased embryonic lethality of *adam9/12/15/17*$^{-/-}$ mice compared with *adam17*$^{-/-}$ mice (Table III) remains to be determined. Images of fixed and hematoxylin and eosin–stained heart sections mounted in Permount/Histoclear were acquired with Axiovision software via an Axiocam HRC camera mounted on an Axioplan2 microscope (software, camera, and microscope all from Carl Zeiss MicroImaging, Inc.). The objective was a Plan-Neofluar 10×/0,30 (44 03 30; Carl Zeiss MicroImaging, Inc.) lens. Images were processed with Adobe Photoshop® 7.0, and the surface area of heart valves in serial sections was measured using NIH Image 1.63 software.

Expression vectors for AP-tagged EGFR ligands

Plasmids encoding AP-tagged EGFR ligands were constructed by inserting partial cDNAs for human TGFα, amphiregulin, epiregulin, EGF, betacellulin, and HB-EGF into the 3′ end of human placental AP cDNA on a pRc/CMV-based expression vector pAIPh. pAIPh contains an NH_2-terminally located HB-EGF signal sequence. In all cases, the junction between AP and the EGFR ligand was placed next to the membrane-proximal EGF repeat. Release of the AP module into the culture supernatant thus requires cleavage at the COOH-terminal cleavage site. It should be noted that the results obtained with AP-tagged EGFR ligands corroborate previous results that TGFα, HB-EGF, and amphiregulin are cleaved by ADAM17 (Peschon et al., 1998; Merlos-Suarez et al., 2001; Sunnarborg et al., 2002; Jackson et al., 2003). This validates the use of AP tags to measure ectodomain shedding for these substrates. In addition, the use of an AP tag has been independently validated using the TNF family members TNFα and TRANCE/OPGL (Zheng et al., 2002; Chesneau et al., 2003). This strongly suggests that an AP tag, which provides a sensitive and quantitative means of measuring ectodomain shedding, should not interfere with the shedding properties of the other EGFR ligands tested here.

Generation of primary MEFs

Primary MEFs were generated from wild-type or *adam*$^{-/-}$ E13.5 embryos and were cultured as described previously (Weskamp et al., 2002). In ad-

dition to *adam9/12/15*$^{-/-}$ triple knockout and *adam9/12/15/17*$^{-/-}$ quadruple knockout mice, we also used *adam17*$^{-/-}$ (Peschon et al., 1998) and *adam19*$^{-/-}$ (Zhou et al., 2004) mice as well as wild-type controls of mixed genetic background (129Sv/C57Bl6) to generate the corresponding primary mEF cells. All genotyping was performed by Southern blot analysis. *adam10*$^{-/-}$ fibroblast cell lines derived from E9.5 embryos have been described previously (Hartmann et al., 2002).

Northern blot analyses

Procedures for isolation of mRNA, gel electrophoresis, transfer to membranes, and generation of ^{32}P-labeled cDNA probes of the indicated ADAMs under high stringency were described previously (Weskamp and Blobel, 1994).

Transfections and shedding assays

cDNA constructs encoding AP-EGFR ligand fusion proteins were transfected with LipofectAMINE™ (Invitrogen). Fresh Opti-MEM (Invitrogen) medium was added the next day, incubated for 1 h, and then replaced with fresh medium containing either 20 ng/ml PMA or 1 μM batimastat (provided by D. Becherer, GlaxoSmithKline, Research Triangle Park, NC), which was also collected after 1 h. Evaluation of AP activity by SDS-PAGE or by colorimetric assays was performed as described previously (Zheng et al., 2002). No AP activity was present in conditioned media of nontransfected cells.

Western blot analysis

Western blot analysis of the expression of ADAM10 and ADAM17 in MEFs and in different mouse tissues was performed as described previously (Weskamp et al., 1996). The blots were probed with a polyclonal antiserum against ADAM10 (CHEMICON International) and against ADAM17 (Schlöndorff et al., 2000).

Statistical analyses

t tests for two samples assuming equal variances were used to calculate the P values. P values <0.05 were considered statistically significant.

We are grateful to Dr. Atsuko Fujisawa-Sehara for providing *adam12*$^{-/-}$ mice; to Drs. Valerie Chesneau, Roy Black, Graham Carpenter, and Peter Dempsey for critical comments on the manuscript; and to Thadeous Kacmarczyk for excellent technical assistance.

This work was supported by National Institutes of Health grant RO1 GM65740 (to C.P. Blobel), by the Memorial Sloan-Kettering Cancer Center support grant NCI-P30-CA-08748, and by the Samuel and May Rudin Foundation, the DeWitt Wallace Fund, the Fonds der Chemischen Industrie, and the Deutsche Forschungsgemeinschaft.

Submitted: 21 July 2003
Accepted: 13 January 2004

References

Asakura, M., M. Kitakaze, S. Takashima, Y. Liao, F. Ishikura, T. Yoshinaka, H. Ohmoto, K. Node, K. Yoshino, H. Ishiguro, et al. 2002. Cardiac hypertrophy is inhibited by antagonism of ADAM12 processing of HB-EGF: metalloproteinase inhibitors as a new therapy. *Nat. Med.* 8:35–40.

Black, R.A., and J.M. White. 1998. ADAMs: focus on the protease domain. *Curr. Opin. Cell Biol.* 10:654–659.

Borrell-Pages, M., F. Rojo, J. Albanell, J. Baselga, and J. Arribas. 2003. TACE is required for the activation of the EGFR by TGF-α in tumors. *EMBO J.* 22: 1114–1124.

Brachmann, R., P.B. Lindquist, M. Nagashima, W. Kohr, T. Lipari, M. Napier, and R. Derynck. 1989. Transmembrane TGF-α precursors activate EGF/TGF-α receptors. *Cell.* 56:691–700.

Chesneau, V., D. Becherer, Y. Zheng, H. Erdjument-Bromage, P. Tempst, and C.P. Blobel. 2003. Catalytic properties of ADAM19. *J. Biol. Chem.* 278: 22331–22340.

Cohen, S. 1962. Isolation of a mouse submaxillary gland protein accelerating incisor eruption and eyelid opening in the new-born animal. *J. Biol. Chem.* 237: 1555–1562.

Cohen, S. 1965. The stimulation of epidermal proliferation by a specific protein (EGF). *Dev. Biol.* 12:394–407.

de Larco, J.E., and G.J. Todaro. 1978. Growth factors from murine sarcoma virus-transformed cells. *Proc. Natl. Acad. Sci. USA.* 75:4001–4005.

Dempsey, P.J., K.S. Meise, Y. Yoshitake, K. Nishikawa, and R.J. Coffey. 1997. Apical enrichment of human EGF precursor in Madin-Darby canine kidney cells involves preferential basolateral ectodomain cleavage sensitive to a metalloprotease inhibitor. *J. Cell Biol.* 138:747–758.

Derynck, R., A.B. Roberts, M.E. Winkler, E.Y. Chen, and D.V. Goeddel. 1984. Human transforming growth factor-α: precursor structure and expression in *E. coli*. *Cell.* 38:287–297.

Dong, J., L.K. Opresko, P.J. Dempsey, D.A. Lauffenburger, R.J. Coffey, and H.S. Wiley. 1999. Metalloprotease-mediated ligand release regulates autocrine signaling through the epidermal growth factor receptor. *Proc. Natl. Acad. Sci. USA.* 96:6235–6240.

Ghiglione, C., E.A. Bach, Y. Paraiso, K.L. Carraway, III, S. Noselli, and N. Perrimon. 2002. Mechanism of activation of the *Drosophila* EGF receptor by the TGFα ligand Gurken during oogenesis. *Development.* 129:175–186.

Gschwind, A., S. Hart, O.M. Fischer, and A. Ullrich. 2003. TACE cleavage of proamphiregulin regulates GPCR-induced proliferation and motility of cancer cells. *EMBO J.* 22:2411–2421.

Harris, R.C., E. Chung, and R.J. Coffey. 2003. EGF receptor ligands. *Exp. Cell Res.* 284:2–13.

Hartmann, D., B. de Strooper, L. Serneels, K. Craessaerts, A. Herreman, W. Annaert, L. Umans, T. Lubke, A. Lena Illert, K. von Figura, and P. Saftig. 2002. The disintegrin/metalloprotease ADAM 10 is essential for Notch signalling but not for α-secretase activity in fibroblasts. *Hum. Mol. Genet.* 11: 2615–2624.

Higashiyama, S., J.A. Abraham, J. Miller, J.C. Fiddes, and M. Klagsbrun. 1991. A heparin-binding growth factor secreted by macrophage-like cells that is related to EGF. *Science.* 251:936–939.

Hooper, N.M., E.H. Karran, and A.J. Turner. 1997. Membrane protein secretases. *Biochem. J.* 321:265–279.

Horiuchi, K., G. Weskamp, L. Lum, H.P. Hammes, H. Cai, T.A. Brodie, T. Ludwig, R. Chiusaroli, R. Baron, K.T. Preissner, et al. 2003. Potential role for ADAM15 in pathological neovascularization in mice. *Mol. Cell. Biol.* 23: 5614–5624.

Iwamoto, R., S. Yamazaki, M. Asakura, S. Takashima, H. Hasuwa, K. Miyado, S. Adachi, M. Kitakaze, K. Hashimoto, G. Raab, et al. 2003. Heparin-binding EGF-like growth factor and ErbB signaling is essential for heart function. *Proc. Natl. Acad. Sci. USA.* 100:3221–3226.

Izumi, Y., M. Hirata, H. Hasuwa, R. Iwamoto, T. Umata, K. Miyado, Y. Tamai, T. Kurisaki, A. Sehara-Fujisawa, S. Ohno, and E. Mekada. 1998. A metalloprotease-disintegrin, MDC9/meltrin-gamma/ADAM9 and PKCdelta are involved in TPA-induced ectodomain shedding of membrane-anchored heparin-binding EGF-like growth factor. *EMBO J.* 17:7260–7272.

Jackson, L.F., T.H. Qiu, S.W. Sunnarborg, A. Chang, C. Zhang, C. Patterson, and D.C. Lee. 2003. Defective valvulogenesis in HB-EGF and TACE-null mice is associated with aberrant BMP signaling. *EMBO J.* 22:2704–2716.

Kurisaki, T., A. Masuda, K. Sudo, J. Sakagami, S. Higashiyama, Y. Matsuda, A. Nagabukuro, A. Tsuji, Y. Nabeshima, M. Asano, et al. 2003. Phenotypic analysis of Meltrin α (ADAM12)-deficient mice: involvement of Meltrin α in adipogenesis and myogenesis. *Mol. Cell. Biol.* 23:55–61.

Lee, J.R., S. Urban, C.F. Garvey, and M. Freeman. 2001. Regulated intracellular ligand transport and proteolysis control EGF signal activation in *Drosophila*. *Cell.* 107:161–171.

Lemjabbar, H., and C. Basbaum. 2002. Platelet-activating factor receptor and ADAM10 mediate responses to *Staphylococcus aureus* in epithelial cells. *Nat. Med.* 8:41–46.

Lemjabbar, H., D. Li, M. Gallup, S. Sidhu, E. Drori, and C. Basbaum. 2003. Tobacco smoke-induced lung cell proliferation mediated by tumor necrosis factor α-converting enzyme and amphiregulin. *J. Biol. Chem.* 278:26202–26207.

Mann, G.B., K.J. Fowler, A. Gabriel, E.C. Nice, R.L. Williams, and A.R. Dunn. 1993. Mice with a null mutation of the TGF α gene have abnormal skin architecture, wavy hair, and curly whiskers and often develop corneal inflammation. *Cell.* 73:249–261.

Massague, J., and A. Pandiella. 1993. Membrane-anchored growth factors. *Annu. Rev. Biochem.* 62:515–541.

Merlos-Suarez, A., S. Ruiz-Paz, J. Baselga, and J. Arribas. 2001. Metalloprotease-dependent protransforming growth factor-α ectodomain shedding in the absence of tumor necrosis factor-α-converting enzyme. *J. Biol. Chem.* 276: 48510–48517.

Miettinen, P.J., J.E. Berger, J. Meneses, Y. Phung, R.A. Pedersen, Z. Werb, and R. Derynck. 1995. Epithelial immaturity and multiorgan failure in mice lacking epidermal growth factor receptor. *Nature.* 376:337–341.

Peschon, J.J., J.L. Slack, P. Reddy, K.L. Stocking, S.W. Sunnarborg, D.C. Lee,

W.E. Russel, B.J. Castner, R.S. Johnson, J.N. Fitzner, et al. 1998. An essential role for ectodomain shedding in mammalian development. *Science.* 282: 1281–1284.

Prenzel, N., E. Zwick, H. Daub, M. Leserer, R. Abraham, C. Wallasch, and A. Ullrich. 1999. EGF receptor transactivation by G-protein-coupled receptors requires metalloproteinase cleavage of proHB-EGF. *Nature.* 402:884–888.

Primakoff, P., and D.G. Myles. 2000. The ADAM gene family: surface proteins with an adhesion and protease activity packed into a single molecule. *Trends Genet.* 16:83–87.

Schlöndorff, J., and C.P. Blobel. 1999. Metalloprotease-disintegrins: modular proteins capable of promoting cell-cell interactions and triggering signals by protein ectodomain shedding. *J. Cell Sci.* 112:3603–3617.

Schlöndorff, J., J.D. Becherer, and C.P. Blobel. 2000. Intracellular maturation and localization of the tumour necrosis factor α convertase (TACE). *Biochem. J.* 347:131–138.

Seals, D.F., and S.A. Courtneidge. 2003. The ADAMs family of metalloproteases: multidomain proteins with multiple functions. *Genes Dev.* 17:7–30.

Shilo, B.Z. 2003. Signaling by the *Drosophila* epidermal growth factor receptor pathway during development. *Exp. Cell Res.* 284:140–149.

Shing, Y., G. Christofori, D. Hanahan, Y. Ono, R. Sasada, K. Igarashi, and J. Folkman. 1993. Betacellulin: a mitogen from pancreatic beta cell tumors. *Science.* 259:1604–1607.

Shoyab, M., G.D. Plowman, V.L. McDonald, J.G. Bradley, and G.J. Todaro. 1989. Structure and function of human amphiregulin: a member of the epidermal growth factor family. *Science.* 243:1074–1076.

Sibilia, M., and E.F. Wagner. 1995. Strain-dependent epithelial defects in mice lacking the EGF receptor. *Science.* 269:234–238.

Strachan, L., J.G. Murison, R.L. Prestidge, M.A. Sleeman, J.D. Watson, and K.D. Kumble. 2001. Cloning and biological activity of epigen, a novel member of the epidermal growth factor superfamily. *J. Biol. Chem.* 276:18265–18271.

Sunnarborg, S.W., C.L. Hinkle, M. Stevenson, W.E. Russell, C.S. Raska, J.J. Peschon, B.J. Castner, M.J. Gerhart, R.J. Paxton, R.A. Black, and D.C. Lee. 2002. Tumor necrosis factor-α converting enzyme (TACE) regulates epidermal growth factor receptor ligand availability. *J. Biol. Chem.* 277: 12838–12845.

Suzuki, T., Q. Yan, and W.J. Lennarz. 1998. Complex, two-way traffic of molecules across the membrane of the endoplasmic reticulum. *J. Biol. Chem.* 273: 10083–10086.

Threadgill, D.W., A.A. Dlugosz, L.A. Hansen, T. Tennenbaum, U. Lichti, D. Yee, C. LaMantia, T. Mourton, K. Herrup, R.C. Harris, et al. 1995. Targeted disruption of mouse EGF receptor: effect of genetic background on mutant phenotype. *Science.* 269:230–234.

Todaro, G.J., C. Fryling, and J.E. De Larco. 1980. Transforming growth factors produced by certain human tumor cells: polypeptides that interact with epidermal growth factor receptors. *Proc. Natl. Acad. Sci. USA.* 77:5258–5262.

Tokumaru, S., S. Higashiyama, T. Endo, T. Nakagawa, J. Miyagawa, K. Yamamori, Y. Hanakawa, H. Ohmoto, K. Yoshino, Y. Shirakata, et al. 2000. Ectodomain shedding of epidermal growth factor receptor ligands is required for keratinocyte migration in cutaneous wound healing. *J. Cell Biol.* 151:209–220.

Toyoda, H., T. Komurasaki, D. Uchida, Y. Takayama, T. Isobe, T. Okuyama, and K. Hanada. 1995. Epiregulin. A novel epidermal growth factor with mitogenic activity for rat primary hepatocytes. *J. Biol. Chem.* 270:7495–7500.

Tsruya, R., A. Schlesinger, A. Reich, L. Gabay, A. Sapir, and B.Z. Shilo. 2002. Intracellular trafficking by Star regulates cleavage of the *Drosophila* EGF receptor ligand Spitz. *Genes Dev.* 16:222–234.

Urban, S., J.R. Lee, and M. Freeman. 2001. *Drosophila* rhomboid-1 defines a family of putative intramembrane serine proteases. *Cell.* 107:173–182.

Urban, S., J.R. Lee, and M. Freeman. 2002. A family of Rhomboid intramembrane proteases activates all *Drosophila* membrane-tethered EGF ligands. *EMBO J.* 21:4277–4286.

Weskamp, G., and C.P. Blobel. 1994. A family of cellular proteins related to snake venom disintegrins. *Proc. Natl. Acad. Sci. USA.* 91:2748–2751.

Weskamp, G., J.R. Krätzschmar, M. Reid, and C.P. Blobel. 1996. MDC9, a widely expressed cellular disintegrin containing cytoplasmic SH3 ligand domains. *J. Cell Biol.* 132:717–726.

Weskamp, G., H. Cai, T.A. Brodie, S. Higashyama, K. Manova, T. Ludwig, and C.P. Blobel. 2002. Mice lacking the metalloprotease-disintegrin MDC9 (ADAM9) have no evident major abnormalities during development or adult life. *Mol. Cell. Biol.* 22:1537–1544.

Wong, S.T., L.F. Winchell, B.K. McCune, H.S. Earp, J. Teixido, J. Massague, B. Herman, and D.C. Lee. 1989. The TGF-α precursor expressed on the cell surface binds to the EGF receptor on adjacent cells, leading to signal transduction. *Cell.* 56:495–506.

Yamazaki, S., R. Iwamoto, K. Saeki, M. Asakura, S. Takashima, A. Yamazaki, R. Kimura, H. Mizushima, H. Moribe, S. Higashiyama, et al. 2003. Mice with defects in HB-EGF ectodomain shedding show severe developmental abnormalities. *J. Cell Biol.* 163:469–475.

Yan, Y., K. Shirakabe, and Z. Werb. 2002. The metalloprotease Kuzbanian (ADAM10) mediates the transactivation of EGF receptor by G protein–coupled receptors. *J. Cell Biol.* 158:221–226.

Yarden, Y., and M.X. Sliwkowski. 2001. Untangling the ErbB signalling network. *Nat. Rev. Mol. Cell Biol.* 2:127–137.

Zheng, Y., J. Schlöndorff, and C.P. Blobel. 2002. Evidence for regulation of the tumor necrosis factor α-convertase (TACE) by protein-tyrosine phosphatase PTPH1. *J. Biol. Chem.* 277:42463–42470.

Zhou, H.M., G. Weskamp, V. Chesneau, U. Sahin, A. Vortkamp, K. Horiuchi, R. Chiusaroli, R. Hahn, D. Wilkes, P. Fisher, et al. 2004. Essential role for ADAM19 in cardiovascular morphogenesis. *Mol. Cell. Biol.* 24:96–104.

THE JOURNAL OF BIOLOGICAL CHEMISTRY
Vol. 279, No. 45, Issue of November 5, pp. 47335–47343, 2004
Printed in U.S.A.

Suppression of the Biological Activities of the Epidermal Growth Factor (EGF)-like Domain by the Heparin-binding Domain of Heparin-binding EGF-like Growth Factor*

Received for publication, July 28, 2004, and in revised form, August 23, 2004
Published, JBC Papers in Press, August 24, 2004, DOI 10.1074/jbc.M408556200

Risa Takazaki, Yuji Shishido‡, Ryo Iwamoto§, and Eisuke Mekada

From the Department of Cell Biology, Research Institute for Microbial Diseases, Osaka University, 3-1, Yamadaoka, Suita, Osaka 565-0871, Japan

Heparin-binding EGF-like growth factor (HB-EGF) is a member of the EGF family of growth factors that has a high affinity for heparin and heparan sulfate. While interactions with heparin are thought to modulate the biological activity of HB-EGF, the precise role of the heparin-binding domain has remained unclear. We analyzed the activity of wild-type HB-EGF and a mutant form lacking the heparin-binding domain (ΔHB) in the presence or absence of heparin. The activity of the EGF-like domain of HB-EGF was determined by measuring binding to diphtheria toxin (DT) as well as the growth factor activity in EGF receptor-expressing cells. The binding affinity of ΔHB for DT was much higher than that of wild-type HB-EGF in the absence of heparin. The binding affinity of HB-EGF for DT was increased by addition of exogenous heparin and reached the level close to the affinity of ΔHB, whereas that of ΔHB was not affected. Moreover, the growth factor activity of ΔHB was much higher than that of wild-type HB-EGF in the absence of heparin but was not affected by addition of exogenous heparin, whereas HB-EGF had increased growth factor activity with added heparin. These results indicate that the heparin-binding domain suppresses the activity of the EGF-like domain of HB-EGF and that association of heparin with HB-EGF via this domain removes the suppressive effect. Thus, we conclude that the heparin-binding domain serves as a negative regulator of this growth factor.

Cell surface heparan sulfate proteoglycans (HSPGs)[1] have been implicated in a variety of cell signaling pathways involving heparin-binding growth factors or cytokines. These growth factors and cytokines form tight complexes with heparin and HSPGs, an interaction that has critical effects on the signaling activity of the ligand (1). Among the ligands known to bind to heparin or heparan sulfate are the fibroblast growth factor (FGF) family of growth factors (2), the transforming growth factor-β family of growth factors (3), vascular endothelial growth factor (4), interleukin-3 (5), granulocyte-macrophage colony-stimulating factor (5), interferon-γ (6), Hedgehog (7), and Wnt (7). Many classes of receptors, including receptor serine/threonine kinases and seven pass transmembrane receptors, have now been shown to be modulated by HSPGs (1). Binding of ligand to cell surface HS is thought to result in a high local ligand concentration to activate signaling receptors. Although biochemical and cell culture data suggest that this binding usually facilitates but is not essential for ligand-receptor interactions and signaling, in the case of Wnt and Hedgehog, HSPGs are crucial for proper pathway function during development (8). Studies with FGFs and their receptor tyrosine kinases also documented a coreceptor role for HSPGs and have suggested models in which HS promotes ligand dimerization, leading to receptor dimerization and stimulation of kinase activity (1).

Heparin-binding EGF-like growth factor (HB-EGF), a member of the EGF family growth factors, has a high affinity for heparin and heparan sulfate (HS) (9, 10). HB-EGF is first synthesized as a type I transmembrane protein (pro-HB-EGF) containing heparin-binding and EGF-like domains (9, 11). Pro-HB-EGF is cleaved within the juxtamembrane domain on the cell surface, resulting in the shedding of soluble HB-EGF (sHB-EGF) (12), which acts as a mitogenic signal through the EGF receptor (EGFR) (9). Pro-HB-EGF is biologically active as a juxtacrine growth factor that signals to neighboring cells in a nondiffusible manner (13–15). Pro-HB-EGF forms complexes with CD9 (13, 16–18) and integrin $\alpha_3\beta_1$ (19) on the cell membrane and acts as a receptor for diphtheria toxin (DT), mediating the entry of DT into the cytoplasm (18, 20). sHB-EGF is a potent mitogen and chemoattractant for a number of cell types, including vascular smooth muscle cells, fibroblasts, and keratinocytes (10, 21). HB-EGF has been implicated in a number of physiological and pathological processes, which include wound healing (22, 23), cardiac hypertrophy (24), smooth muscle cell hyperplasia (25), kidney collecting duct morphogenesis (26), blastocyst implantation (27), pulmonary hypertension (28), and oncogenic transformation (29). In addition, we recently demonstrated through analysis of HB-EGF null mice that HB-EGF is an essential factor for normal heart function and valvulogenesis (30).

The modulation of various HB-EGF activities by cell surface HSPGs has been previously described (21). For examples: (i) reduced HS expression on the cell surface decreases the ability of HB-EGF to stimulate the migration of bovine aortic smooth muscle cells (10), (ii) binding of HB-EGF to HSPG-deficient CHO cells expressing EGFR is lower than binding to wild-type

* This work was supported by a Grant-in-aid from the Ministry of Education, Culture, Sports, Science, and Technology (14580696 to R. I.) and by a Grant-in-aid from Japan Society for the Promotion of Science (16-8487 to R. T.). The costs of publication of this article were defrayed in part by the payment of page charges. This article must therefore be hereby marked "*advertisement*" in accordance with 18 U.S.C. Section 1734 solely to indicate this fact.

‡ Present address: Brain Research Institute, Niigata University, Niigata 951-8585, Japan.

§ To whom correspondence should be addressed. Tel.: 81-6-6879-8288; Fax: 81-6-6879-8289; E-mail: riwamoto@biken.osaka-u.ac.jp.

[1] The abbreviations used are: HSPGs, heparan sulfate proteoglycans; HS, heparan sulfate; FGF; fibroblast growth factor; HB-EGF, heparin-binding epidermal growth factor-like growth factor; EGF, epidermal growth factor; R, receptor; DT, diphtheria toxin; CHO, Chinese hamster ovary; CM, conditioned medium; sHB-EGF, soluble HB-EGF; DER, 32D-EGFR.

CHO cells expressing EGFR, an effect that is rescued by the addition of exogenous heparin (31), (iii) CHO cells expressing pro-HB-EGF, but deficient in cell surface HSPGs, were 15-fold less sensitive to DT-toxicity than wild-type CHO cells, but DT sensitivity was restored by addition of either HS or heparin, which increased the binding affinity of pro-HB-EGF for DT (32). Although previous studies well documented the modulation of the biological activities of HB-EGF with heparin, the precise role of the heparin-binding domain remained unclear. Here we analyze the DT binding and growth factor activities of HB-EGF and a mutant form lacking the heparin-binding domain, in the presence or absence of heparin. We present evidence that the heparin-binding domain of HB-EGF suppresses the activity of the EGF-like domain and that binding of heparin to this domain removes the suppressive effect.

EXPERIMENTAL PROCEDURES

Materials—DT was produced as previously described (33). Heparin sodium salt (from bovine intestinal mucosa) was purchased from Sigma. Heparitinase (EC 4.2.2.8, catalog no. 100703) was purchased from Seikagaku Co. (Tokyo, Japan). Heparin-Sepharose CL-6B was purchased from Amersham Biosciences. TALON metal affinity resin was purchased from Clontech Laboratory, Inc. (Palo Alto, CA). Anti-human HB-EGF-neutralizing antibody was purchased from R&D Systems (Minneapolis, MN). Anti-human HB-EGF (H6) antibody was prepared as previously described (18). Anti-human EGFR antibody (1005) was purchased from Santa Cruz Biotechnology, Inc. (Santa Cruz, CA). Anti-phospho-EGFR (Tyr-1068) antibody was purchased from Cell Signaling Technology, Inc. (Beverly, MA).

Generation of HB-EGF Mutant Constructs—cDNA encoding a mutant form of sHB-EGF lacking the heparin-binding domain ($HB^{\Delta tm\Delta hb}$) was obtained and isolated by PCR using the forward primer (5′-GACCCATGTCTTCGGAAATACAAG-3′) and the phosphorylated reverse primer (5′-CCCGTGCTCCTCCTTGTTTGGTGT-3′), using $pRcHB^{\Delta tm}$, which contains the human HB-EGF deletion mutant ($HB^{\Delta tm}$) missing the transmembrane and cytoplasmic domains (34), as a template. This amplified fragment was self-ligated, generating the $pRcHB^{\Delta tm\Delta hb}$ construct. $pRcHB^{\Delta tm}$ and $pRcHB^{\Delta tm\Delta hb}$ were digested with HindIII and XbaI. The digested cDNA fragment containing $HB^{\Delta tm}$ or $HB^{\Delta tm\Delta hb}$ was then ligated into the HindIII/XbaI sites of pcDNA6/myc-His (Invitrogen Corp., San Diego, CA), generating the pcDNA6/$HB^{\Delta tm}$myc-His and pcDNA6/$HB^{\Delta tm\Delta hb}$myc-His constructs, respectively. The cDNA encoding the heparin-binding domain deletion mutant of pro-HB-EGF (pro-$HB^{\Delta hb}$) was obtained and isolated by PCR using the same primer set as above and using pRcHB-EGF, which contains the entire human pro-HB-EGF coding region (18), as a template. This amplified fragment was self-ligated, generating the pRcpro-$HB^{\Delta hb}$ construct. The integrity of all constructs was verified by sequencing.

Cell Culture and Transfection—DER cells, murine 32D hematopoietic progenitor cells stably expressing human EGFR (14), were maintained as previously described (14). Both the CHO mutant cell line pgsD-677 (also known as 677) and the 677H cell line (677 cells stably expressing pro-HB-EGF) (32) were maintained as previously described (32). Stable transfectants of L cells, including LH cells stably expressing pro-HB-EGF, and LC cells stably expressing CD9 (18), were maintained as previously described (18). To obtain transfectants producing human sHB-EGF and sΔHB, 677 cells were transfected with plasmids encoding sHB-EGF cDNA (pcDNA6/$HB^{\Delta tm}$myc-His) or sΔHB cDNA (pcDNA6/$HB^{\Delta tm\Delta hb}$myc-His) using LipofectAMINE 2000 (Invitrogen) according to the manufacturer's instructions. 24 h after transfection, the medium was exchanged with fresh RPMI1640 containing 10% fetal calf serum, and cells were cultured for 48 h. Conditioned medium (CM) containing sHB-EGF or sΔHB was harvested and centrifuged. To obtain stable transfectants of 677 cells and L cells that express pro-ΔHB, cells were transfected with pRcpro-$HB^{\Delta hb}$ by the calcium phosphate method (35). Cells were cultured for 48 h and further cultured for 7 days in the presence of 200 μg/ml G418. Colonies growing in the selection medium were isolated and assayed for DT-binding activity as described later. Positive clones were isolated and subcloned again. Clones with highest expression of human pro-ΔHB were chosen from among 677pro-ΔHB cells derived from 677 cells and Lpro-ΔHB cells derived from L cells.

Immunoblotting of HB-EGF—Recombinant His-tagged sHB-EGF and sΔHB proteins were collected from conditioned medium of transfected 677 cells using TALON metal affinity resin. Samples were boiled in SDS-PAGE sample buffer with 10% 2-mercaptoethanol, run on an SDS-PAGE gel, and transferred to an Immobilon membrane (Millipore Corp., Bedford, MA). The membrane was blocked with 1% skim milk in TTBS (0.05% Tween 20, 20 mM Tris, pH 7.5, 0.15 M NaCl), incubated with anti-human HB-EGF-neutralizing antibody followed by horseradish peroxidase-conjugated anti-goat IgG antibody. Proteins were visualized using an ECL Western blotting kit (Amersham Biosciences).

To detect pro-HB-EGF and pro-ΔHB protein in transfected 677 cell lysates, cells were lysed with OG-lysis buffer (60 mM 1-*O*-*n*-octyl-β-D-glucopyranoside, 0.15 M NaCl, 20 mM Hepes-NaOH, pH 7.2, 10 mM EDTA, 0.5 μM phenylmethylsulfonyl fluoride, 0.15 μM aprotinin, 1 μM E-64, 1 μM leupeptin) and then centrifuged for 20 min at 15,000 × *g*. The supernatant was boiled in SDS-PAGE sample buffer with 10% 2-mercaptoethanol and then run on an SDS-PAGE gel and transferred to an Immobilon membrane. After blocking with 1% skim milk in TTBS, the membrane was incubated with anti-human HB-EGF-neutralizing antibody and then incubated with horseradish peroxidase-conjugated anti-goat IgG antibody. The membrane was finally analyzed using an ECL Western blotting kit.

Heparin-Sepharose Chromatography—CM samples containing sHB-EGF or sΔHB were diluted by 2-fold with the dilution buffer (20 mM HEPES-NaOH, pH 7.2). 10 μl of heparin-Sepharose was added to 900 μl of the diluted sample, and the mixture was incubated at 4 °C for 4 h. The incubated heparin-Sepharose was washed three times with 1 ml of washing buffer (50 mM NaCl, 20 mM HEPES-NaOH, pH 7.2), and eluted with 50 μl of elution buffer (0.05–1.65 M NaCl and 20 mM HEPES, pH 7.2). Equal amounts of eluants were boiled in SDS-PAGE sample buffer with 10% 2-mercaptoethanol and then run on an SDS-PAGE gel and transferred to an Immobilon membrane. The membrane was blotted with anti-human HB-EGF-neutralizing antibody and with horseradish peroxidase-conjugated anti-goat IgG antibody as described above.

DT Binding Assay—Purified DT was labeled with $Na^{125}I$ (Amersham Biosciences) by an IODO-GEN Pre-Coated Iodination Tube (Pierce) according to the manufacturer's instructions. Binding of ^{125}I-DT to sHB-EGF secreted into CM was measured as follows: 500 μl of CM containing either sHB-EGF or sΔHB, both His-tagged, was added to 20 μl of 1 M HEPES-NaOH, pH 7.2, and then the mixture was incubated with 20 μl of TALON metal affinity resin at 4 °C for 4 h. After washing the gel three times with 1 ml WS buffer (0.1% bovine serum albumin in phosphate-buffered saline), the gel was suspended with 970 μl of WS buffer. Then the gel was incubated with 10 μl of ^{125}I-DT at the indicated concentrations in the presence or absence of 10 μl of unlabeled DT (final 10 μg/ml) and 10 μl of heparin at the indicated concentrations. After incubation for 8 h at 4 °C, the gel was washed three times with 1 ml of WS buffer. The radioactivity bound to the gel was counted with a γ-counter. Specific binding of ^{125}I-DT to the recombinant HB-EGF molecules was calculated by subtracting the radioactivity of a sample with excess unlabeled DT from that of the sample without unlabeled DT. Specific binding values were plotted as described by Scatchard (36) to determine the number of DT binding sites and the binding affinity of sHB-EGF or sΔHB for DT. Binding curves were generated by regression analysis.

Binding of ^{125}I-DT to pro-HB-EGF at the cell surface was measured as previously described (18), except that 100 ng/ml ^{125}I-DT was used. This concentration (1.7 nM) is close to the concentration required for half-saturation of DT binding to human pro-HB-EGF (18, 37). Nonspecific binding of ^{125}I-DT was assessed in the presence of 10 μg/ml unlabeled DT. Specific binding was determined by subtracting the nonspecific binding from the total binding obtained using ^{125}I-DT alone. The relative values of ^{125}I-DT binding to pro-HB-EGF and to pro-ΔHB on the cell surface were calculated as the ratio of specific DT binding to the total amount of pro-HB-EGF or pro-ΔHB on the cell surface, measured by the anti-HB-EGF antibody (H-6) binding assay, as previously described (38).

Determination of the Concentration of sHB-EGF and sΔHB in the CM Samples—The concentration of sHB-EGF and sΔHB in each CM sample was calculated from the B_{max} value in the Scatchard plot analysis of DT binding as described above. In each experiment, the actual concentration was determined in which the B_{max} value was corrected by a proportion of collected recombinant protein with the metal affinity resin, by using a known concentration of commercial purified recombinant HB-EGF (R&D Systems) as a standard. CM samples determined for the concentrations of these species were used in the mitogenic assay and in the EGFR autophosphorylation assay as described later.

Heparitinase Treatments of Cells—Heparitinase treatments were carried out as described previously (32).

Mitogenic Assay—40 μl of DER cells (1.0×10^4 cells) in RPMI 1640 containing 10% fetal calf serum were inoculated in each well of a 96-well tissue culture plate. CM samples containing either sHB-EGF or

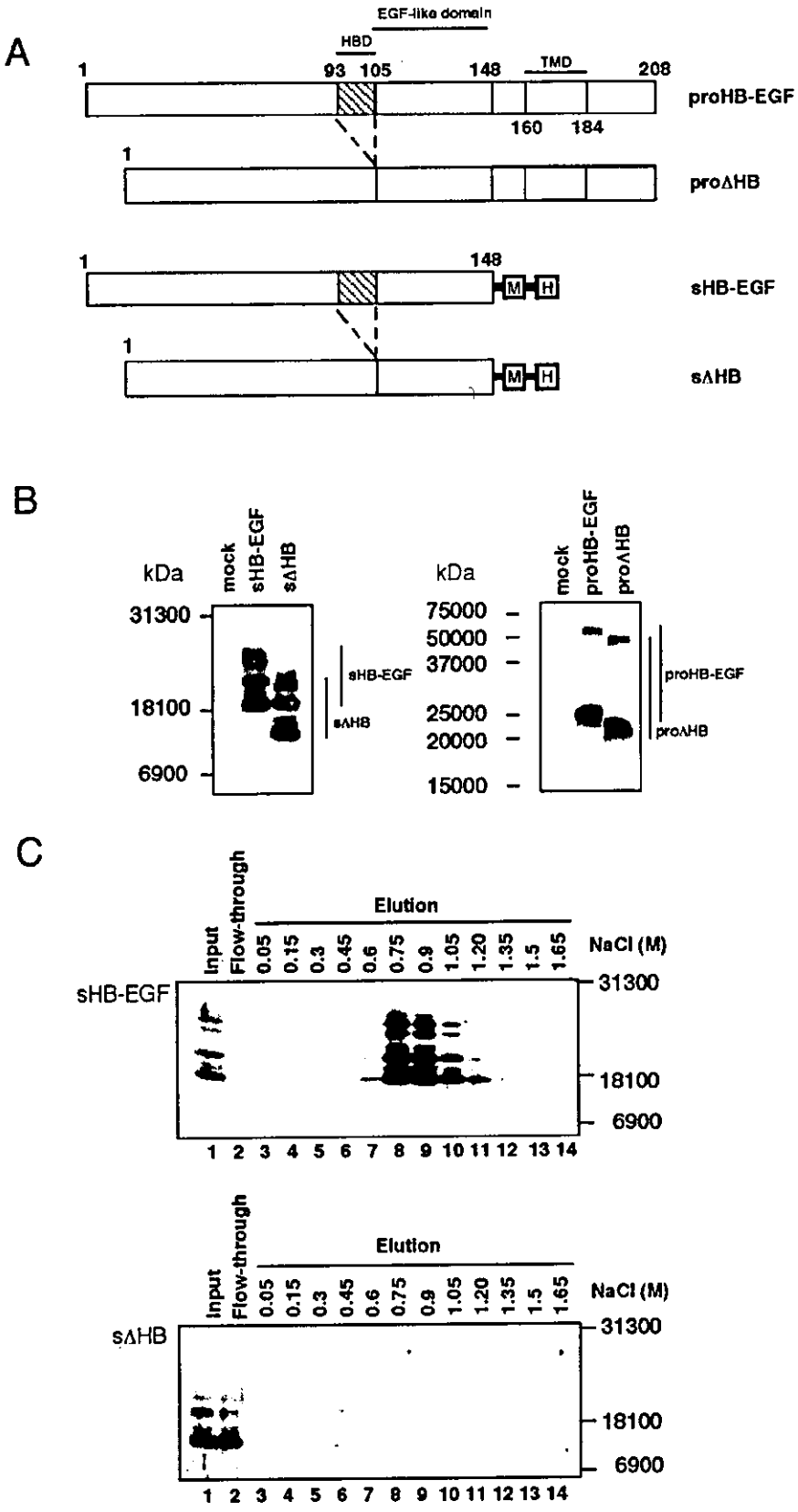

FIG. 1. **Characterization of the mutant forms of HB-EGF lacking the heparin-binding domain.** *A*, schematic structures of wild-type and mutant forms of HB-EGF. *pro-HB-EGF*, full-length membrane-anchored HB-EGF; *pro-ΔHB*, deletion mutant of pro-HB-EGF lacking the heparin-binding domain; *sHB-EGF*, myc- and His-tagged mutant of pro-HB-EGF with transmembrane and cytoplasmic domain truncation; *sΔHB*, myc- and His-tagged deletion mutant of sHB-EGF lacking heparin-binding domain; *HBD*, heparin-binding domain; *TMD*, transmembrane domain; *M*, myc tag; *H*, His tag. *B*, Western blot analysis detecting sHB-EGF and sΔHB in the culture medium (*left panel*) and pro-HB-EGF and pro-ΔHB in the cell lysates (*right panel*) of transfected 677 cells. HB-EGF species were detected by immunoblotting using anti-HB-EGF-neutralizing antibody. *C*, heparin-Sepharose chromatography of sHB-EGF (*upper*) and sΔHB (*lower*). sHB-EGF was able to bind to the heparin-Sepharose column and was eluted by >0.75 M NaCl, whereas sΔHB did not show any binding to heparin-Sepharose, and almost all sΔHB input was detected in the flow-through fraction.

sΔHB were diluted with the medium to the indicated concentrations. 50 μl of CM sample, with or without anti-HB-EGF-neutralizing antibody (10 μg/ml), was added to the wells containing the DER cells. 10 μl of heparin at the indicated concentrations was also added to the wells. After 36 h of culture at 37 °C, the cell number in each well was measured by the Cell Count Reagent SF (Nacalai, Kyoto, Japan), according to the manufacturer's instructions. The mitogenic activity of the secreted HB-EGF species was calculated as the difference between the